Mathematics and Mechanics of Solids

http://mms.sagepub.com

Structured Deformations as Energy Minimizers in Models of Fracture and Hysteresis

R. Choksi, G. Del Piero, I. Fonseca and D. Owen

Mathematics and Mechanics of Solids 1999; 4; 321
DOI: 10.1177/108128659900400304

The online version of this article can be found at:
http://mms.sagepub.com/cgi/content/abstract/4/3/321

Published by:

http://www.sagepublications.com

Additional services and information for *Mathematics and Mechanics of Solids* can be found at:

Email Alerts: http://mms.sagepub.com/cgi/alerts

Subscriptions: http://mms.sagepub.com/subscriptions

Reprints: http://www.sagepub.com/journalsReprints.nav

Permissions: http://www.sagepub.co.uk/journalsPermissions.nav

Citations http://mms.sagepub.com/cgi/content/refs/4/3/321

Downloaded from http://mms.sagepub.com at SIMON FRASER LIBRARY on November 11, 2008

Structured Deformations as Energy Minimizers in Models of Fracture and Hysteresis

R. CHOKSI
Department of Mathematics and Statistics, Simon Fraser University, Barnaby, British Columbia V5S 156, Canada

G. DEL PIERO
Istituto di Ingegneria, Università Degli Studi di Ferrara, Via Saragat, 1 44100 Ferrara, Italy

I. FONSECA
D. OWEN
Department of Mathematical Sciences, Carnegie Mellon University, Pittsburgh, PA 15213, USA

(Received 29 May 1998; Final version 13 July 1998)

Abstract: This paper reviews recent theories of nonclassical, structured deformations and integral representations for their Helmholtz free energy. Energy minimizers for a body undergoing shearing at two different length scales and for a bar experiencing both smooth extension and macroscopic fractures are determined, and applications to the shearing of single crystals and to the cohesive fracture of solids are discussed. Yield, hysteresis, and the associated dissipation in two-level shears are shown to arise from instabilities at the micro level, and the dichotomy between brittle and ductile fracture is related precisely to a critical length of a bar.

1. INTRODUCTION

Structured deformations [1, 2] provide a geometrical setting rich enough to include smooth, classical deformations, which underlie much of solid and fluid mechanics, and piecewise smooth deformations, which describe macroscopic cracking as studied in fracture mechanics, as well as the complex combination of macroscopic and microscopic changes relevant for the study of liquid crystals, crystals with defects, and granular materials. The variety of geometrical changes described by structured deformations offers many mechanisms for lowering the energy of a body. Thus, the determination of metastable equilibrium configurations of a body entails the resolution of complex competitions between smooth deformations and nonsmooth "disarrangements" [3] at both macroscopic and microscopic length scales. For example, in a metallic solid, separation of a crack at a single site at the macro level can compete with lattice distortions and slip at many sites at the micro level to determine how the solid responds to prescribed tractions and displacements.

In the context of complex geometrical changes at more than one length scale, it is essential to have a rational procedure for assigning an energy to each structured deformation. In Choksi and Fonseca [4], a procedure is set forth that permits one to determine the bulk and interfacial

Mathematics and Mechanics of Solids, **4**: 321-356, 1999
© 1999 Sage Publications, Inc.

Downloaded from http://mms.sagepub.com at SIMON FRASER LIBRARY on November 11, 2008

from the SAGE Social Science Collections. All Rights Reserved.

densities of the (Helmholtz) free energy associated with each structured deformation, given the corresponding free energy densities for each piecewise classical, simple deformation [1]. The results obtained in [4] show that the bulk density of free energy of a structured deformation can be influenced by the bulk density and by the interfacial density of free energy for simple deformations that approximate the given structured deformation. Moreover, precise relations among these densities are derived in [4] via tools from geometric measure theory and the calculus of variations.

In Sections 2 and 3, we summarize the geometry and the energetics of structured deformations, and we employ this framework in Sections 4 and 5 to predict in simple models the onset and detailed features of fracture, yielding, and hysteresis.

In Section 2.1, we describe the basic concepts and principal results for structured deformations in the original setting studied in [1, 2]. In Section 2.2, we reexamine these concepts in a broader mathematical setting employing functions of special bounded variation, functions that arise naturally in applications based on the calculus of variations [4]. In this setting, a counterpart [4, Theorem 2.12] of the approximation theorem [1, Theorem 5.8] forms the basis for the definition of the energy of a structured deformation. In turn, the formulas for bulk and interfacial free energy density given in Section 3 provide the basis for the analysis of fracture and hysteresis in Sections 4 and 5. The reader interested mainly in these applications may wish to skip the material in Sections 2.2 and 3 on a first reading of this paper.

In Section 4, we address the competition between shearing at two different length scales to determine the equilibrium configurations of a body at fixed temperature. In Section 4.1, we consider a two-dimensional body that undergoes special structured deformations called two-level shears. Macroscopically, each two-level shear is a simple shear of amount μ, called the macroshear. A microview of a two-level shear reveals small, thin, parallel rectangular bodies that undergo individually a simple shear of amount γ, called the shear without slip. The difference $\mu - \gamma$ is shown to be a volume density of deformation due to microslip and is called the shear due to microslip. The definition of a structured deformation in Section 2.1 permits μ and γ to be arbitrary real numbers, and the representation of the bulk free energy density provided in Section 3 tells us that this density H for a two-level shear is a function of μ and of γ. Under special circumstances described at the end of Section 3, this function reduces to the sum of a function of γ alone and a function of $\mu - \gamma$ alone:

$$H(\mu, \gamma) = \varphi(\gamma) + \psi(\mu - \gamma). \tag{1}$$

When applied to a single crystal that can deform through lattice distortion and through slips concentrated within slip bands, the term $\varphi(\gamma)$ in (1) is the free energy associated with smooth distortion of the crystal lattice, and the term $\psi(\mu - \gamma)$ is the free energy associated with the slips of parts of the lattice relative to other parts that accumulate across slip bands. These interpretations lead us to assume that φ is a nonnegative, smooth, strictly convex function and that ψ is a nonnegative, smooth, periodic function whose period p is interpreted and estimated in Section 4.3.

In Section 4.1, we find for each $\mu \in \mathbb{R}$ the local minimizers of the function $\gamma \longmapsto \varphi(\gamma) + \psi(\mu - \gamma)$; that is, we find the (meta)stable two-level shearing configurations of a rectangular block when the macroshear μ is prescribed. We show that the stable equilibrium pairs (μ, γ) consist of a countable number of bounded, smooth S-shaped curves in the μ-

Downloaded from http://mms.sagepub.com at SIMON FRASER LIBRARY on November 11, 2008

γ plane (Figure 5), called stable branches. We demonstrate in Sections 4.1 and 4.2 how the geometry of the stable branches is compatible with the phenomenon of hysteresis, when pairs (μ,γ) are permitted not only to move continuously along stable branches but to jump vertically from a point of one stable branch to a point on another stable branch (Figure 6). Each vertical jump between stable branches corresponds to a sudden redistribution of the current macroshear μ between the shear without microslip γ and the shear due to microslip $\mu-\gamma$. As we show in Section 4.2, this redistribution of shear is the source of hysteresis and dissipation for two-level shears under prescribed macroshear.

We examine also in Sections 4.1 and 4.2 the problem of determining the local minimizers of the function $(\mu,\gamma) \longmapsto \varphi(\gamma)+\psi(\mu-\gamma)-\sigma\mu$, with σ a given real number. This corresponds to finding the (meta)stable two-level shearing configurations of a bar under prescribed shearing traction σ. As shown in Section 4.1, the stable pairs (μ,γ) form a proper subset of the stable pairs under prescribed macroshear, with each stable branch now ending at points where the tangent line is horizontal and where the shear without microslip attains an absolute maximum or an absolute minimum value (Figure 7). We show how the geometry of the stable branches is compatible with yielding and hysteresis, when pairs (μ,γ) now are permitted to jump horizontally from an endpoint of one stable branch to an endpoint of another. In each horizontal jump to the right from a maximum of γ, and in each horizontal jump to the left from a minimum of γ, the free energy does not change and the work done is positive. Such horizontal jumps between neighboring branches are dissipative and irreversible. In spite of the irreversibility of these jumps, the original stable branch can be reached again from a neighboring branch by first moving the pair (μ,γ) along the neighboring stable branch so as to change γ from its maximum to its minimum value (or vice versa), and then undergoing a horizontal jump back to the original stable branch. In this manner, the phenomena of yielding and hysteresis are compatible with the two-level shearing of a bar under prescribed shearing tractions (Figure 8). Both phenomena arise through transitions between unstable pairs at the ends of stable branches of the equilibrium locus. These transitions may be described as material instabilities at the micro level.

In Section 4.3, we examine the physical setting of a single crystal with specific choices of the free energy densities φ and ψ. Experiments show that families of parallel slip bands with separations on the order of 10^4 atomic units support the deformation due to microslip, and we indicate how this fact fixes the period p of the microslip energy density ψ at the value 10^{-4}. Our simple model predicts that irreversible shearing deformation due to microslip can occur only in integral multiples of 10^{-4}; changes in microslip of magnitude less than 10^{-4} correspond to reversible movement of the pair (μ,γ) on a single stable branch. The choice made for φ implies that the traction σ and the shear without microslip γ satisfy the linear relation $\sigma = k\gamma$, with $k = \varphi''(\gamma)$ at a stable equilibrium triple (μ,γ,σ), so that $(\mu,\gamma) = (\mu,\frac{\sigma}{k})$. Thus, the stable branches in the μ-γ plane are necessarily the stable branches of the stress-strain relation $\left\{(\mu,\sigma) \mid (\mu,\frac{\sigma}{k},\sigma) \text{ is a stable triple}\right\}$. To within a rescaling of the vertical axis by a factor of k, the curves in Figure 8 describe the stress-strain relation for a bar undergoing two-level shear under prescribed traction and for the choices of free energy densities φ and ψ made in Section 4.3. In this subsection, we also calculate and compare numerical values of the ratio φ/ψ at the onset of shearing and at yield.

Downloaded from http://mms.sagepub.com at SIMON FRASER LIBRARY on November 11, 2008

In contrast to the competition between shearing without slip and shearing due to microslip studied in Section 4, we turn our attention in Section 5 to the competition between one-dimensional smooth stretching of a bar and one-dimensional cohesive fracture of the bar. Thus, we focus on the following questions: at what value of stretch, if any, during the smooth extension of a bar does the formation of one or more cracks become energetically favorable, and, if cracks do form, what occurs after their formation?

In Section 5.1, we consider simple deformations with energy

$$E(f) = \int_0^l W(\nabla f(x))\,dx + \sum_{z \in \Gamma(f)} \Theta([f](z)) \tag{2}$$

given as a sum of two parts, a bulk part with density W depending on the gradient of the macroscopic deformation and an interfacial part concentrated at the jump set $\Gamma(f)$ and expressed by the values of a function Θ of the jumps. The bulk density W is assumed to be strictly convex. To reflect the assumed cohesive nature of fracture as described in the model of Barenblatt [5], we assume that the function Θ is increasing and strictly concave. We consider here only the case of a bar in a hard device for which the deformed length βl is specified, with β a given positive number.

In Sections 5.1 and 5.2, we consider the first and second variations of the energy (2) of the bar constrained by the hard device and obtain both necessary and sufficient conditions for a given simple deformation to be a local minimizer. Two of the necessary conditions that we establish are statements of uniformity of the deformation: ∇f and $[f]$ must be constant. Therefore, the energy at stationary points takes the simple form

$$E(f) = lW(\nabla f) + n\Theta([f]), \tag{3}$$

with n the number of jumps, and the deformed length of the bar is given by

$$l\nabla f + n[f] = \beta l. \tag{4}$$

The assumptions made on the function Θ imply the inequality $\Theta(n[f]) \leq n\Theta([f])$, and this tells us that it is energetically favorable to replace n small cracks of a single size by one large crack n times that size. In other words, a metastable configuration of the bar must have at most one crack, so that $n = 0$ or $n = 1$. In the case of extension, $\beta \geq 1$, a local minimizer must satisfy $1 \leq \nabla f \leq \beta$.

These considerations lead us to seek local minimizers of the function $\nabla f \longmapsto lW(\nabla f) + \Theta(l(\beta - \nabla f))$ on the interval $[0, \beta]$. The analysis carried out in Section 5.2 yields the locus of pairs $(\nabla f, \beta)$ that correspond to metastable equilibria of the bar (Figures 10 and 11). Two cases can occur, depending on whether the undeformed length l of the bar exceeds or is less than a critical length l_c determined by the functions W and Θ. For the case $l > l_c$, the stable branches are as shown in Figure 10, and there is a distinguished value of the extension β below which no fracture occurs and above which a crack of size no less than a specific positive amount must form. This case is referred to as brittle fracture, since the distribution of deformation between smooth extension and cracking changes abruptly at the distinguished value of the extension. For the case $l \leq l_c$, the stable branches are given in Figure 11, and

Downloaded from http://mms.sagepub.com at SIMON FRASER LIBRARY on November 11, 2008

there again is a distinguished value of the extension β below which no fracture occurs. As β increases through this value, a crack does open, but the amount of opening increases gradually from the value 0 as β increases above the distinguished value. Thus, when the undeformed length of the bar exceeds the critical length, for small extensions it is energetically favorable to have no cracks and for large extensions it is energetically favorable to have one crack whose minimum size is positive. When the undeformed length of the bar is no greater than the critical length, at small extensions it is again energetically favorable to have no cracks, but for large extensions it is energetically favorable to have one crack whose size increases gradually from zero with the amount of extension. This case is referred to as ductile fracture because of the gradual increase in crack size. The analysis in Section 5.2 also provides us with the stress extension diagrams for both brittle fracture and ductile fracture (Figure 12). Finally, in Section 5.3, we discuss the relationship between our results and other research on fracture.

We have shown that the energetics of structured deformations given in Sections 2 and 3 is consistent with the phenomena of yield, hysteresis, brittle fracture, and ductile fracture. The analysis of the examples in Section 4, to model a competition between shearing without microslip and shearing due to microslip, and in Section 5, to model a competition between smooth stretching and cohesive fracture of a bar, encourages us to believe that a more systematic incorporation of the theory of structured deformations into continuum mechanics may enable us to describe and to predict a wider class of phenomena of interest in contemporary materials science.

2. GEOMETRY OF STRUCTURED DEFORMATIONS

2.1. Structured Deformations

In this subsection, we follow the description of structured deformations contained in [1–3], presenting the essential definitions and results. We begin by making explicit the classes of regions that bodies can occupy in the N-dimensional Euclidean space $\mathcal{E}$. According to Noll and Virga [6], a fit region $\mathcal{A}$ is a bounded, regularly open subset of $\mathcal{E}$ with finite perimeter and whose boundary has zero volume. A piecewise fit region [1] is a finite union of (not necessarily disjoint) fit regions. The definition of a structured deformation rests on two special kinds of deformations: classical deformations and simple deformations. A classical deformation from a fit region $\mathcal{A}$ is an orientation-preserving mapping $f : \mathcal{A} \to \mathcal{E}$ that extends to all of $\mathcal{E}$ as a C^1 mapping that is invertible and whose inverse is of class C^1. A simple deformation is a piecewise classical deformation in the following sense: a simple deformation from a piecewise fit region $\mathcal{A}$ is a pair (κ, f), with κ a subset of $\mathcal{A}$ and f a mapping from $\mathcal{A}\backslash\kappa$ into $\mathcal{E}$ such that κ has volume zero, f is injective, and $\mathcal{A}\backslash\kappa$ is a finite union of fit regions from each of which f is a classical deformation. The set κ is called the disarrangement site, and the mapping f is called the transplacement for the simple deformation (κ, f). (In [1], κ is called the crack site; the more comprehensive term disarrangement was introduced in [3].)

A structured deformation (κ, g, G) from a piecewise fit region $\mathcal{A}$ consists of a simple deformation (κ, g) from $\mathcal{A}$ and a continuous tensor field $G : \mathcal{A}\backslash\kappa \to Lin\mathcal{V}$ (with $\mathcal{V}$ the translation space of $\mathcal{E}$ and $Lin\mathcal{V}$ the set of all linear mappings on $\mathcal{V}$) such that

Downloaded from http://mms.sagepub.com at SIMON FRASER LIBRARY on November 11, 2008

1. G is piecewise continuous on the closure of $\mathcal{A}$; that is, there exists a finite collection of fit regions $\{\mathcal{A}_j : j \in \{1, \cdots, J\}\}$ whose union is $\mathcal{A}\backslash\kappa$ and for each of which $G|_{\mathcal{A}_j}$ extends continuously to the closure of $\mathcal{A}_j$
2. there exists a positive number m for which

$$m \leq \det G(x) \leq \det \nabla g(x) \tag{5}$$

for all x in $\mathcal{A}\backslash\kappa$.

The definition of structured deformation by itself provides no interpretation for the tensor field G, but an interpretation is provided by the approximation theorem [1]: every structured deformation (κ, g, G) from $\mathcal{A}$ is a limit of simple deformations from $\mathcal{A}$, in the sense that there exists a sequence $n \longmapsto (\kappa_n, f_n)$ of simple deformations such that

$$g = \lim_{n\to\infty} f_n \tag{6}$$

$$G = \lim_{n\to\infty} \nabla f_n \tag{7}$$

and

$$\kappa = \liminf_{n\to\infty} \kappa_n . \tag{8}$$

In (6) and (7), the limits are taken in the sense of L^∞ convergence, and in (8), $\liminf_{n\to\infty} \kappa_n := \bigcup_{n=1}^{\infty} \bigcap_{p=n}^{\infty} \kappa_p$. The relations (6)-(8) identify each ingredient in a structured deformation (κ, g, G) in terms of the disarrangement sites, transplacements, and gradients of transplacements associated with a sequence of simple deformations $n \longmapsto (\kappa_n, f_n)$. These identification relations justify our calling κ the (permanent) disarrangement site, g the transplacement, and G the deformation without disarrangements: $G(x)$ represents the local deformation at x without including the effects of discontinuities of the transplacements f_n at the disarrangement sites κ_n for the approximating simple deformations (κ_n, f_n). In the limit as n tends to infinity, some of the points of the disarrangement sites κ_n occur repeatedly as members of the disarrangement site κ, and some diffuse away from κ throughout subregions of $\mathcal{A}$. Moreover, the limit in (7) permits us to interpret deformations associated with G as occurring away from the disarrangement sites κ_n in smaller and smaller pieces of the body; that is,

$$G(x) = \lim_{r\to 0} \lim_{n\to\infty} \mathcal{L}^N(\mathcal{B}(x,r))^{-1} \int_{\mathcal{B}(x,r)\backslash\kappa_n} \nabla f_n(y)\, dy \tag{9}$$

for all $x \in \mathcal{A}\backslash\kappa$, where $\mathcal{B}(x,r)$ is the ball centered at x of radius r and $\mathcal{L}^N$ denotes the Lebesgue measure in the N-dimensional space $\mathcal{E}$. By contrast, we call ∇g and g the macroscopic local deformation and the macroscopic transplacement for the structured deformation (κ, g, G); they are encountered in classical descriptions of the geometrical

Downloaded from http://mms.sagepub.com at SIMON FRASER LIBRARY on November 11, 2008

changes in a continuous body, whereas G reflects geometrical changes at smaller length scales that we interpret as changes in geometry at the micro level.

The identification relations (6)-(8) permit one to deduce an identification relation for the tensor field $M := \nabla g - G$ [2]: for each structured deformation (κ, g, G) and for each sequence $n \longmapsto (\kappa_n, f_n)$ satisfying (6)-(8), the relation

$$M(x) = \lim_{r\to 0}\lim_{n\to\infty} \mathcal{L}^N\,(\mathcal{B}(x,r))^{-1} \int_{\Gamma(f_n)\cap\mathcal{B}(x,r)} [f_n](y)\otimes \nu(y)\, dH^{N-1}(y) \tag{10}$$

holds for every $x \in \mathcal{A}\backslash\kappa$. Here, $\Gamma(f_n)$ is the set of jump points of f_n, $[f_n](y)$ is the jump of f_n at y, $\nu(y)$ is the unit normal to $\Gamma(f_n)$ at a point y in $\Gamma(f_n)$, and H^{N-1} denotes the $(N-1)$-dimensional Hausdorff measure in $\mathcal{E}$. Note that $\mathcal{L}^3$ and H^2 are the usual volume and area measures in three-dimensional Euclidean space. It was observed in [2] that relation (10) identifies M as the volume density of deformation due to discontinuities in transplacements at the micro level, and we call M the deformation due to microdisarrangements. (The term deformation due to microfracture was used in [1].) Thus, the algebraically obvious identity

$$\nabla g = G + M \tag{11}$$

has the deeper significance of an additive decomposition of the macroscopic deformation ∇g into the deformation without disarrangements G and the deformation due to microdisarrangements M.

We close this subsection by noting that $\det G$ is the volume change without disarrangements, whereas $\det \nabla g$ represents the macroscopic volume change. Thus, the second inequality in (5) expresses the condition that disarrangements can only increase or maintain volumes. This condition is necessary in order that the transplacements f_n approximating g be injective and, hence, not cause interpenetration of matter [1]. Of course, the equality

$$\det G = \det \nabla g \tag{12}$$

expresses the condition that no volume changes occur through disarrangements.

2.2. Structured Deformations in the Context of SBV

We begin this subsection with an intuitive discussion of the spaces BV and SBV. The reader familiar with these spaces is encouraged to skip to the definition of structured deformations in the paragraph preceding relation (14).

In Section 3, we will give meaning to the energy of a structured deformation (κ, g, G). In view of the approximation theorem [1], given an approximating sequence of simple deformations $n \mapsto (\kappa_n, f_n)$, it is natural to consider the limit

$$\lim_{n\to\infty} (\text{bulk energy of } f_n + \text{interfacial energy of } f_n)\,. \tag{13}$$

Downloaded from http://mms.sagepub.com at SIMON FRASER LIBRARY on November 11, 2008

An approximating sequence is far from unique, and an energetically obvious selection rests on the least costly sequences $n \mapsto (\kappa_n, f_n)$ realizing the infimum of (13) over all possible sequences that approximate (κ, g, G). What can be said about this infimum and its dependence on the pair (g, G)? Characterizations of integral representations have been the focus of extensive research in recent years and require thorough manipulations of approximating sequences. To pursue such analysis, it becomes necessary to relax the regularity and convergence assumptions of (6), (7), and (8). Moreover, with the possibility of interpreting fields as limits of local averages of quantities at small length scales (see (9) and (10)), it is natural to work with function spaces and topologies that center not on pointwise behavior but on averaging properties. Thus, it proves both useful and natural to generalize the notion of a structured deformation and to weaken the pointwise convergence in (6) and (7).

Just as generalizations of continuous and smooth functions may be provided by L^p and Sobolev functions, a natural extension of the space of discontinuous, piecewise smooth functions is BV, the space of functions of bounded variation. Functions of bounded variation are functions whose weak (distributional) derivative is a measure. A piecewise smooth function u is in BV, and its distributional derivative comprises two parts: a bulk part representing the gradient away from the disarrangement site and a singular part consisting of a surface-like measure supported on the interface where the jump discontinuity occurs. This singular measure contains information about both the area of the disarrangement site and the amplitude of the disarrangement.

Of course, the space BV includes functions that are not piecewise smooth, and this fact presents two potential difficulties. One is that the singular part of the derivative may consist of a measure supported on a fractional dimensional set; that is, a measure associated with neither the bulk nor jump derivatives. Such behavior is exemplified by the Cantor-Vitali function defined on the unit interval [0,1], an increasing continuous function whose "bulk" derivative is zero (i.e., its graph has slope of zero at almost every point) but whose distributional derivative is a positive measure supported on the Cantor middle-third set. By removing such functions from BV, one obtains SBV, the set of functions of special bounded variation [9]. Functions in SBV are truly generalizations of piecewise smooth functions, as the singular part of their distributional derivative is supported exactly on the set where the function experiences jump discontinuities. For this reason, the space SBV is sufficiently large to provide an excellent working environment. The second difficulty is that, even within the SBV setting, jump discontinuities in a deformation u can be dense and the bulk part of the derivative, written ∇u, may lose completely its curl-free structure.

To provide a broader setting for structured deformations (κ, g, G), we shall consider the transplacement g to be in SBV, and we shall assume the deformation without disarrangements G to be an integrable tensor field. To give a precise description of the space SBV, we let $\Omega \subset \mathbb{R}^N$ be an open, bounded set (with the Euclidean space $\mathcal{E}$ now identified with $\mathbb{R}^N$), and we recall that a function $u \in L^1(\Omega; \mathbb{R}^N)$ is said to be of bounded variation, $u \in BV(\Omega; \mathbb{R}^N)$, if for all $i \in \{1, \ldots, N\}, j \in \{1, \ldots, N\}$, there exists a finite Radon measure μ_{ij} such that

$$\int_\Omega u_i(x) \frac{\partial \varphi}{\partial x_j}(x)\, d\mathcal{L}^N(x) = -\int_\Omega \varphi(x)\, d\mu_{ij}$$

Downloaded from http://mms.sagepub.com at SIMON FRASER LIBRARY on November 11, 2008

for every $\varphi \in C_0^1(\Omega;\mathbb{R})$. Equivalently, $u \in BV(\Omega;\mathbb{R}^N)$ if its distributional derivative Du is a Radon measure with finite total variation. It can be shown that $Du = (\mu_{ij})$ may be represented as the sum of three mutually singular measures: if $U \subset \Omega$ is an open set, then

$$Du(U) = \int_U \nabla u(x) d\mathcal{L}^N(x) + \int_{\Gamma(u)\cap U} [u](x) \otimes \nu(x) dH^{N-1}(x) + C(u)(U),$$

where ∇u is the density of the absolutely continuous part of Du with respect to $\mathcal{L}^N$, u^+ and u^- are the traces of u on the jump set $\Gamma(u)$, and $[u] := u^+ - u^-$ is the jump of u across $\Gamma(u)$. $C(u)$ is the so-called Cantor part of the measure Du; its support has Hausdorff dimension between $N-1$ and N. We also write

$$Du = \nabla u \, \mathcal{L}^N + D_s u,$$

with

$$D_s u(U) := \int_{\Gamma(u)\cap U} [u](x) \otimes \nu(x) dH^{N-1}(x) + C(u)(U)$$

for every open set $U \subset \Omega$. If $C(u)$ is the zero measure, then the total variation of Du is given by

$$\|Du\|(\Omega) := \int_\Omega |\nabla u(x)| \, d\mathcal{L}^N(x) + \int_{\Gamma(u)} \left|u^+(x) - u^-(x)\right| dH^{N-1}(x).$$

Although in general $curl\, \nabla u \neq 0$, it is well known that ∇u is an approximate gradient in that near each point x_0 the function u is close, in average, to the affine function $x \mapsto u(x_0) + \nabla u(x_0)(x - x_0)$. Also, $\mathcal{L}^N(\Gamma(u)) = 0$, and $\Gamma(u)$ is $N-1$ rectifiable; that is, there exists a countable family of C^1 hypersurfaces $\{S_k\}_{k=1}^\infty$ such that

$$H^{N-1}(\Gamma(u) \setminus \bigcup_k S_k) = 0.$$

For details, we refer the reader to [7, 8].

In this enlarged setting, the counterparts of simple deformations are functions $u \in BV(\Omega;\mathbb{R}^N)$ that are smooth in the sense that $Du = \nabla u \, \mathcal{L}^N$ or smooth away from a rectifiable set K. In both cases, $C(u) = 0$. The subspace of BV of functions u with $C(u) = 0$, the space of special bounded variation functions, written $SBV(\Omega;\mathbb{R}^N)$, was introduced by De Giorgi and Ambrosio [9].

To introduce structured deformations in this setting, we consider triples (κ, g, G) satisfying

$$g \in SBV(\Omega;\mathbb{R}^N) \qquad \text{and} \qquad G \in L^1(\Omega;\mathbb{M}^{N\times N}),$$

Downloaded from http://mms.sagepub.com at SIMON FRASER LIBRARY on November 11, 2008

with $\mathbb{M}^{N\times N}$ the vector space of $N \times N$ matrices, and satisfying $\kappa \subset \Omega$ with $\mathcal{L}^N(\kappa) = 0$. In particular, structured deformations as defined in Section 2.1 meet these requirements. In the following, we restrict attention to the case where $\kappa = \Gamma(g)$, and we write (g, G) in place of $(\Gamma(g), g, G)$. Following Choksi and Fonseca [4], we call such pairs structured deformations, and we denote by $SD(\Omega)$ the set of all structured deformations.

Using a Lusin-type result due to Alberti [10], Choksi and Fonseca [4] obtained an analog of the approximation theorem of Del Piero and Owen [1]: for each $(g, G) \in SD(\Omega)$, there exists a sequence $n \mapsto f_n$ in $SBV(\Omega; \mathbb{R}^N)$ such that

$$f_n \to g \text{ in } L^1(\Omega; \mathbb{R}^N) \qquad \nabla f_n \overset{*}{\rightharpoonup} G \text{ in the sense of measures.} \tag{14}$$

We write in this case

$$(f_n, \nabla f_n) \rightharpoonup (g, G).$$

Once again, we recover analogs of the identification relations (9) for G and (10) for $M := \nabla g - G$:

$$G(x) = \lim_{r\to 0} \lim_{n\to\infty} \mathcal{L}^N(\mathcal{B}(x,r))^{-1} \int_{\mathcal{B}(x,r)} \nabla f_n(y)\,dy$$

and

$$M(x) = \lim_{r\to 0} \lim_{n\to\infty} \mathcal{L}^N(\mathcal{B}(x,r))^{-1} \int_{\Gamma(u_n)\cap\mathcal{B}(x,r)} [f_n](y) \otimes \nu(y)\, dH^{N-1}(y)$$

for almost every $x \in \Omega$.

Note that we must have $D_s f_n \to (\nabla g - G)\mathcal{L}^N + D_s g$ in the sense of distributions, so if $\nabla g \neq G$, we are forced, whether or not g is in the Sobolev space $W^{1,1}$, to consider in (14) approximating functions $f_n \in SBV \backslash W^{1,1}$. Suppose further that the sequence $n \longmapsto |\nabla f_n|$ is uniformly bounded in L^p for $p > 1$ and that $\sup_n |Df_n|(\Omega) < +\infty$. A compactness theorem for SBV due to Ambrosio [11] implies that, in any open subset E of Ω where $\nabla g(x) \neq G(x)$ for almost every $x \in E$, one must have

$$H^{N-1}(\Gamma(f_n) \cap E) \to \infty \quad \text{as} \quad n \to \infty.$$

We conclude that as n increases, the jump discontinuities of f_n diffuse throughout the part of the region where ∇g differs from G.

3. ENERGETICS

In the sequel, $W : \mathbb{M}^{N\times N} \to [0, +\infty]$ is the bulk energy density and $\Theta : \mathbb{R}^N \times S^{N-1} \to [0, +\infty]$ is the interfacial energy density, where $S^{N-1} := \{\nu \in \mathbb{R}^N : \|\nu\| = 1\}$ is the unit sphere in $\mathbb{R}^N$, and we assign to each $f \in SBV(\Omega; \mathbb{R}^N)$ the energy

Downloaded from http://mms.sagepub.com at SIMON FRASER LIBRARY on November 11, 2008

$$E(f) := \int_{\Omega} W(\nabla f(x))\, d\mathcal{L}^N(x) + \int_{\Gamma(f)} \Theta([f](x), \nu(x))\, dH^{N-1}(x).$$

We seek now to determine from this energy the effective energy of a structured deformation (g, G); that is, the most energetically economical way to realize (g, G) in terms of the energies $E(f_n)$ of approximations $f_n \in SBV(\Omega; \mathbb{R}^N)$. For example, put $\Omega := (0,1)^2$ and consider the pair $(id, \mathbb{I}) \in SD(\Omega)$, with id the identity mapping and $\mathbb{I}$ the 2×2 identity matrix, and put $\Theta(\lambda, \nu) := |\lambda|$. With $f_n = id$ for every n, it is clear that

$$(f_n, \nabla f_n) \rightharpoonup (id, \mathbb{I}) \quad \text{and} \quad E(f_n) = W(\mathbb{I}) \text{ for all } n.$$

On the other hand, if for n even and $(x, y) \in (0,1)^2$, we define

$$\hat{f}_n(x,y) := \begin{cases} (x + \frac{1}{n}, y) & \text{if } \ y \in (\frac{2k}{n}, \frac{2k+1}{n}) \quad \text{and} \quad k \in \{0, 1, \ldots, \frac{n-2}{2}\} \\ (x - \frac{1}{n}, y) & \text{if } \ y \in (\frac{2k+1}{n}, \frac{2k+2}{n}) \quad \text{and} \quad k \in \{0, 1, \ldots, \frac{n-2}{2}\} \end{cases},$$

then

$$(\hat{f}_n, \nabla \hat{f}_n) \rightharpoonup (id, \mathbb{I})$$

and

$$E(\hat{f}_n) = W(\mathbb{I}) + \Theta(\frac{2}{n} e_1, e_2)(n-1) \to W(\mathbb{I}) + 2$$

as $n \to \infty$, where $e_1 = (1, 0)$ and $e_2 = (0, 1)$. This example shows that limits of the energy may depend on the choice of the approximating sequence.

Let $p \in (1, \infty)$ be given. We define the relaxed (or effective) energy $\mathcal{I}(g, G)$ for $(g, G) \in SD(\Omega)$ with $g \in L^\infty(\Omega; \mathbb{R}^N)$ and $G \in L^p(\Omega; \mathbb{M}^{N \times N})$ by

$$\begin{aligned} \mathcal{I}(g, G) \ : \ &= \inf \{ \liminf_{n \to \infty} E(f_n) \ : \ f_n \in SBV(\Omega; \mathbb{R}^N) \text{ for all } n, \\ &\quad (f_n, \nabla f_n) \rightharpoonup (g, G), \ \sup_n |\nabla f_n|_{L^p(\Omega; \mathbb{M}^{N \times N})} < \infty, \ \sup_n |Df_n|(\Omega) < \infty \}. \end{aligned}$$

The argument that established (14) can be used to show that the class of sequences over which this infimum is taken is nonempty. The SBV compactness theorem of Ambrosio prevents us from considering interfacial energy densities Θ that are bounded below by a positive constant. Otherwise, for sequences $n \mapsto f_n$ with bounded energy, we would have $(f_n, \nabla f_n) \rightharpoonup (g, \nabla g)$ and, hence, $\nabla g = G$ almost everywhere. Thus, structured deformations (g, G) with $\nabla g \neq G$ on a set of positive measure would have infinite energy.

In this section, we assume that the bulk and interfacial energy densities W and Θ are continuous and satisfy the following hypotheses:

Downloaded from http://mms.sagepub.com at SIMON FRASER LIBRARY on November 11, 2008

H 1: There exists a constant $K > 0$ such that

$$|W(A) - W(B)| \leq K|A - B| \left(1 + |A|^{p-1} + |B|^{p-1}\right)$$

for all $A, B \in \mathbb{M}^{N\times N}$.

H 2: There exist constants $C, \alpha, L > 0$ such that for all $\lambda \in \mathbb{R}^N$ and $\nu \in S^{N-1}$,

$$0 \leq \Theta(\lambda, \nu) \leq C|\lambda|$$

and

$$\left|\Theta_0(\lambda, \nu) - \frac{\Theta(t\lambda, \nu)}{t}\right| \leq Ct^{\alpha}|\lambda|^{\alpha+1}$$

for every $t \in (0, L)$, where Θ_0, a function that is positively homogeneous of degree one, is defined by

$$\Theta_0(\lambda, \nu) := \limsup_{t\to 0+} \frac{\Theta(t\lambda, \nu)}{t}.$$

H 3: Θ is subadditive. That is, for all $\lambda_1, \lambda_2 \in \mathbb{R}^N$ and $\nu \in S^{N-1}$,

$$\Theta(\lambda_1 + \lambda_2, \nu) \leq \Theta(\lambda_1, \nu) + \Theta(\lambda_2, \nu).$$

Using the blowup method [12], it was shown in [4, Theorem 2.17, Remark 3.3] that for $(g, G) \in SD(\Omega)$ with $G \in L^p(\Omega; \mathbb{M}^{N\times N})$, the energy has the following integral representation:

$$\mathcal{I}(g, G) = \int_{\Omega} H(\nabla g(x), G(x))\, d\mathcal{L}^N(x) + \int_{\Gamma(g)} \chi([g](x))\, dH^{N-1}(x), \tag{15}$$

where for each $A, B \in \mathbb{M}^{N\times N}$, the effective bulk energy density is

$$\begin{aligned} H(A, B) \quad :\quad &= \inf\Big\{ \int_{(0,1)^N} W(\nabla u(x))\, d\mathcal{L}^N(x) + \int_{\Gamma(u)} \Theta_0([u](x), \nu(x))\, dH^{N-1}(x) \ : \\ u \ &\in \ SBV((0,1)^N; \mathbb{R}^N), \quad u|_{\partial(0,1)^N} = x \mapsto Ax, \\ |\nabla u| \ &\in \ L^p((0,1)^N; \mathbb{R})), \int_{(0,1)^N} \nabla u(x)\, d\mathcal{L}^N(x) = B \Big\}. \end{aligned}$$

For $\lambda \in \mathbb{R}^N$, the effective surface energy density becomes

$$\chi(\lambda) \quad :\quad = \inf\Big\{ \int_{\Gamma(u)} \Theta([u](x), \nu(x))\, dH^{N-1}(x) : u \in SBV((0,1)^N; \mathbb{R}^N),$$

Downloaded from http://mms.sagepub.com at SIMON FRASER LIBRARY on November 11, 2008

$$u\,|_{\partial(0,1)^N} = u_{\lambda,e_N}\ ,\ \nabla u = 0\ a.e.\},$$

where

$$u_{\lambda,e_N}\ (x) = \begin{cases} \lambda & if\ \ x\cdot e_N > 0 \\ 0 & if\ \ x\cdot e_N \leq 0. \end{cases}$$

In particular, we remark that the effective bulk energy results from interaction of the initial volume and interfacial energy densities W and Θ, whereas the effective interfacial energy density depends only on the initial interfacial energy Θ.

In the next section, we consider the case in which the effective bulk energy density has the form

$$H(A,B) = \varphi(B) + \psi(A-B). \tag{16}$$

It can be shown that this representation holds in the case where, in addition to the assumptions (H1) – (H3), the function W is given by $W(A) = \frac{K}{2}\,|A-A_0|^2$ for all matrices A and for some $K > 0$ and reference deformation A_0. In this case,

$$H(A,B) = \frac{K}{2}\,|B-A_0|^2 + H(A-B,0) - \frac{K}{2}\,|A_0|^2\,.$$

Moreover, for a bulk energy density W that vanishes at a reference deformation A_0, and for an effective bulk energy H of the form (16), it can be shown that

$$\psi(0) = \varphi(A_0) = 0. \tag{17}$$

4. APPLICATIONS TO HYSTERESIS

4.1. Equilibrium and Hysteresis within the Class of Two-Level Shears

In this subsection, we restrict our attention to structured deformations that describe shears at both macroscopic and microscopic levels. Let μ and γ be real numbers, put $\mathcal{E} = \mathbb{R}^2$, $\mathcal{A} = (0,1)^2$, $\kappa = \emptyset$, and define mappings g and G on $\mathcal{A}$ by

$$g(x,y) \ :\ = (x+\mu y, y) \tag{18}$$

$$G(x,y) \ :\ = \begin{pmatrix} 1 & \gamma \\ 0 & 1 \end{pmatrix} \tag{19}$$

Downloaded from http://mms.sagepub.com at SIMON FRASER LIBRARY on November 11, 2008

It is easy to verify that the triple (κ, g, G) is a structured deformation from $\mathcal{A}$ in the sense of Section 2.1. For this structured deformation, the transplacement is the simple shear g of amount μ, the macroscopic deformation is $\nabla g = \begin{pmatrix} 1 & \mu \\ 0 & 1 \end{pmatrix}$, the deformation without disarrangements is $G = \begin{pmatrix} 1 & \gamma \\ 0 & 1 \end{pmatrix}$, the deformation due to microdiarrangements is $M = \begin{pmatrix} 0 & \mu - \gamma \\ 0 & 0 \end{pmatrix}$, and the (permanent) disarrangement site is $\kappa = \emptyset$. Consequently, the relation (5) is verified with

$$m = \det \begin{pmatrix} 1 & \gamma \\ 0 & 1 \end{pmatrix} = \det \begin{pmatrix} 1 & \mu \\ 0 & 1 \end{pmatrix} = 1. \tag{20}$$

Moreover, if for each positive integer n we put

$$\kappa_n := \left\{ (x, \frac{k}{n}) \,:\, x \in (0,1), k \in \{1, \cdots, n-1\} \right\}$$

and

$$f_n(x,y) := \left(x + \gamma y + \frac{[[ny]]}{n}(\mu - \gamma)\,,\, y \right), \tag{21}$$

then $n \longmapsto (\kappa_n\,, f_n)$ is a sequence of simple deformations that determines the structured deformation (κ, g, G) in the sense that relations (6)-(8) are satisfied. In (21), $[[\cdot]]$ denotes the greatest integer function, and the mapping f_n is a piecewise affine mapping that divides $\mathcal{A}\backslash\kappa_n$ into n horizontal strips, translates each strip to the right an amount $(\mu - \gamma)/n$ relative to the one below it, and shears each strip an amount γ. Thus, the number μ represents the (amount of) shear at the macro level (or, more briefly, the macroshear), the difference $\mu - \gamma$ represents the (amount of) shear due to microslip, and the number γ is the (amount of) shear without microslip. Macro- and microviews of a two-level shear are shown in Figures 1 and 2, respectively.

Because g extends to a smooth mapping on $\mathbb{R}^2$, so that the jump set $\Gamma(g)$ is empty, the representation (15) for the energy of a structured deformation given in Section 3 here takes the form

$$\mathcal{I}(g, G) = \int_{(0,1)^2} H(\nabla g(x), G(x)) d\mathcal{L}^2(x), \tag{22}$$

and we specialize further by assuming the decomposition (16)

$$H(A, B) = \varphi(B) + \psi(A - B). \tag{23}$$

Since ∇g and G are constant fields that depend only on the numbers μ and γ, relations (22) and (23) provide the following formula for the energy of a two-level shear:

$$\mathcal{I}(\mu, \gamma) = \varphi(\gamma) + \psi(\mu - \gamma). \tag{24}$$

Downloaded from http://mms.sagepub.com at SIMON FRASER LIBRARY on November 11, 2008

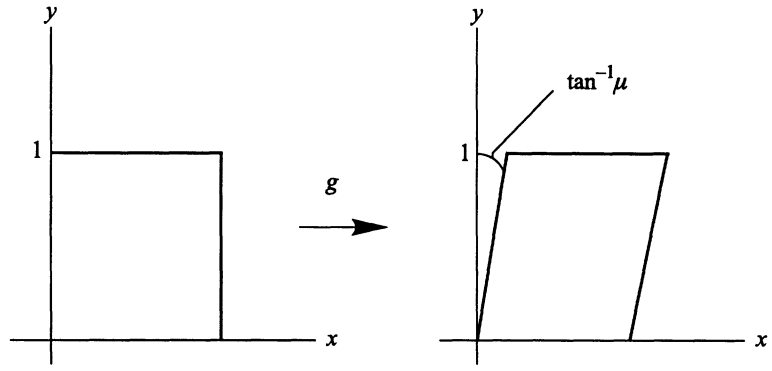

Fig. 1. Macroview of a two-level shear.

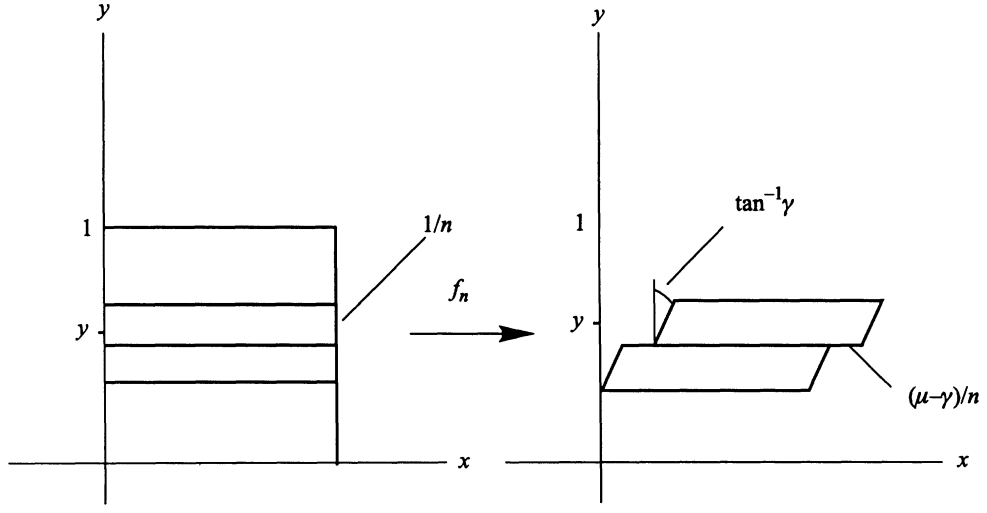

Fig. 2. Microview of a two-level shear.

Downloaded from http://mms.sagepub.com at SIMON FRASER LIBRARY on November 11, 2008

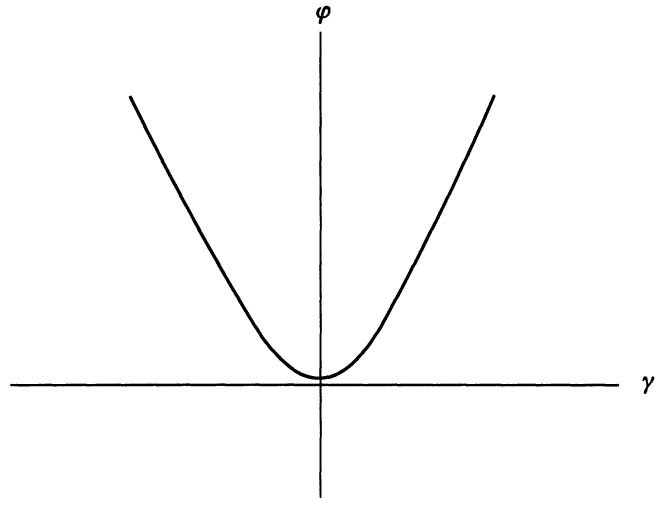

Fig. 3. Lattice energy versus shear without microslip.

For convenience, for the functions occurring in (24), we have used the same symbols as in (22) and (23). In view of the applications to be discussed in Subsection 4.3, we refer to $\varphi(\gamma)$ as the lattice energy density and to $\psi(\mu - \gamma)$ as the microslip energy density for the given two-level shear, and we assume

i. $\varphi : \mathbb{R} \to \mathbb{R}$ is a nonnegative, even function of class C^3 satisfying $\varphi(0) = \varphi'(0) = 0$, $\varphi'''(\gamma) \geq 0$ for all $\gamma \in [0, \infty)$, and there exists $k > 0$ such that $\varphi''(\gamma) \geq k$ for all $\gamma \in \mathbb{R}$

ii. $\psi : \mathbb{R} \to \mathbb{R}$ is a nonnegative, even function of class C^3 that is periodic with period $p > 0$, $\psi(0) = \psi'(0) = \psi''(\frac{p}{4}) = 0$, $\psi''(0) > \varphi''(0)$, $\psi''(s) > 0$ and $\psi'''(s) \leq 0$ for all $s \in (0, \frac{p}{4})$, and

$$\psi(s) = \begin{cases} 2\psi\left(\frac{p}{4}\right) - \psi\left(\frac{p}{2} - s\right) & \text{for} \quad s \in [\frac{p}{4}, \frac{p}{2}) \\ \psi(p - s) & \text{for} \quad s \in [\frac{p}{2}, p). \end{cases} \tag{25}$$

Graphs of energy density functions satisfying (i) and (ii) are illustrated in Figures 3 and 4 (with $\mu - \gamma$ replaced by s in Figure 4).

We now identify within the class of two-level shears the equilibrium configurations of a body whose Helmholtz free energy density in a two-level shear is given by relation (24) and for which either the macroscopic shear μ or the shear stress $\sigma := \sigma_{xy}$ is specified.

CASE 1: In the case where we fix the macroscopic shear μ, we consider the free energy $\mathcal{I}$ in (24) to be a function of γ alone and require for metastable equilibrium that $\mathcal{I}$ have a local minimum. Therefore, we seek values for the shear without microslip γ that satisfy

Downloaded from http://mms.sagepub.com at SIMON FRASER LIBRARY on November 11, 2008

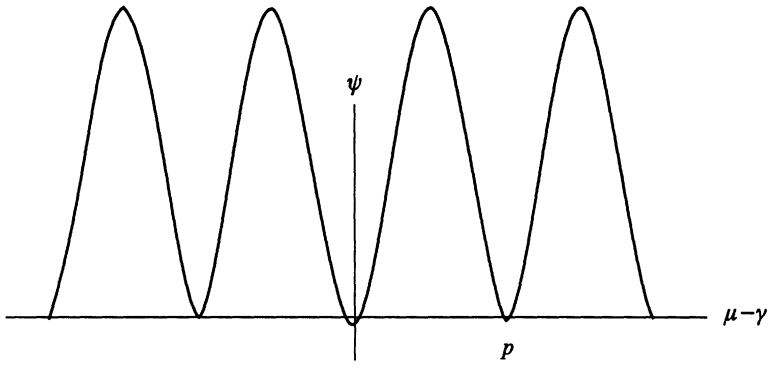

Fig. 4. Microslip energy versus shear due to microslip.

$$\frac{\partial \mathcal{I}}{\partial \gamma} = \varphi'(\gamma) - \psi'(\mu - \gamma) = 0 \tag{26}$$

and

$$\frac{\partial^2 \mathcal{I}}{\partial \gamma^2} = \varphi''(\gamma) + \psi''(\mu - \gamma) > 0. \tag{27}$$

We call pairs (μ, γ) that satisfy (26) stationary pairs, and we note that relation (27) is sufficient in order that the stationarity condition (26) on the energy determines the shear without microslip γ locally as a function of the macroshear μ. When this is the case, we have

$$\frac{\partial \gamma}{\partial \mu} = \frac{\psi''(\mu - \gamma)}{\varphi''(\gamma) + \psi''(\mu - \gamma)}. \tag{28}$$

The assumptions (i) and (ii) on the lattice energy density φ and the microslip energy density ψ imply that there are stationary pairs (μ, γ) that violate (27). The form of the locus of stationary pairs implied by these assumptions is illustrated in Figure 5. The locus divides into branches that alternately satisfy and violate (27), that is, into locally stable branches and unstable branches. In general, the transition between a stable and an unstable branch occurs at stationary pairs (μ, γ) that satisfy

$$\varphi''(\gamma) + \psi''(\mu - \gamma) = 0. \tag{29}$$

According to relation (28), these pairs correspond to points on the locus of stationary pairs at which the tangent line is vertical. Moreover, it is easy to show that the free energy $\mathcal{I}$ attains its global maximum at such pairs, so that $\mathcal{I}$ decreases if γ changes from its value at the stationary pair P in Figure 5 where the tangent line is vertical to its value at the pair Q where the vertical tangent line intersects the nearest stable branch of the locus of stationary pairs. For a deformation process in which the macroshear first is increased, then is decreased, and

Downloaded from http://mms.sagepub.com at SIMON FRASER LIBRARY on November 11, 2008

again is increased, the hysteresis loop shown in Figure 6 is consistent with the requirements that the pair (μ, γ) follow stable branches of the locus of stationary pairs, and, in jumping from one branch to another, the free energy is decreased.

CASE 2: In the case where the shear stress σ on the boundary of the region $\mathcal{A}$ is specified, we take the total energy $\mathcal{E}$ to be the difference

$$\mathcal{E}(\mu, \gamma, \sigma) = \mathcal{I}(\mu, \gamma) - \mu\sigma \tag{30}$$

between the free energy in relation (24) and the work done by the shear stress. We consider now the total energy to be a function of μ and γ and require for equilibrium that $\mathcal{E}$ have a local minimum. Therefore, we seek pairs (μ, γ) that satisfy

$$\frac{\partial \mathcal{E}}{\partial \mu} = \psi'(\mu - \gamma) - \sigma = 0 \tag{31}$$

$$\frac{\partial \mathcal{E}}{\partial \gamma} = \varphi'(\gamma) - \psi'(\mu - \gamma) = 0 \tag{32}$$

and

$$\psi''(\mu - \gamma)\varphi''(\gamma) > 0, \quad \psi''(\mu - \gamma) > 0. \tag{33}$$

The inequalities in (33) express the condition that the Hessian of $\mathcal{E}$ be positive definite, and, in view of the assumption (i) on φ, they are equivalent to the positivity of $\psi''(\mu - \gamma)$. We call pairs (μ, γ) that satisfy (32) stationary pairs, and relations (32) and (26) imply that the locus of stationary pairs (μ, γ) when the shear stress σ is specified is the same as the locus of stationary pairs (33) when the macroshear is specified. However, relations (27) and (33) imply that each stable branch when the shear stress is specified is included in the corresponding stable branch when the macroshear is specified. The transition from stable to unstable branch for specified shear stress occurs when the equilibrium pair (μ, γ) satisfies

$$\psi''(\mu - \gamma) = 0, \tag{34}$$

and inspection of the sign of $\frac{d\gamma}{d\mu}$ in (28), together with relations (34), (32), and the assumption (i), tell us that such transition pairs (μ, γ) must correspond to local maximum and minimum values of the shear without microslip γ . Thus, as is illustrated in Figure 7, the transition pairs between stable and unstable branches are points where the tangent to the stationary locus is horizontal. We note that a jump from one transition pair to a neighboring pair involves no change in the free energy, because γ and, hence, the lattice energy $\varphi(\gamma)$ do not change, and because, from (31), (32), (34), and assumption (ii), $\mu - \gamma$ must change by the period p of the microslip energy ψ. When the shear stress σ and, hence, by (31) and (32), the shear without microslip γ are positive, a horizontal jump to the right from point P in Figure 7 to the neighboring transition pair Q decreases the total energy $\mathcal{E}$, and a horizontal jump to the left from point P to the neighboring transition pair R increases $\mathcal{E}$. When σ is negative, the

Downloaded from http://mms.sagepub.com at SIMON FRASER LIBRARY on November 11, 2008

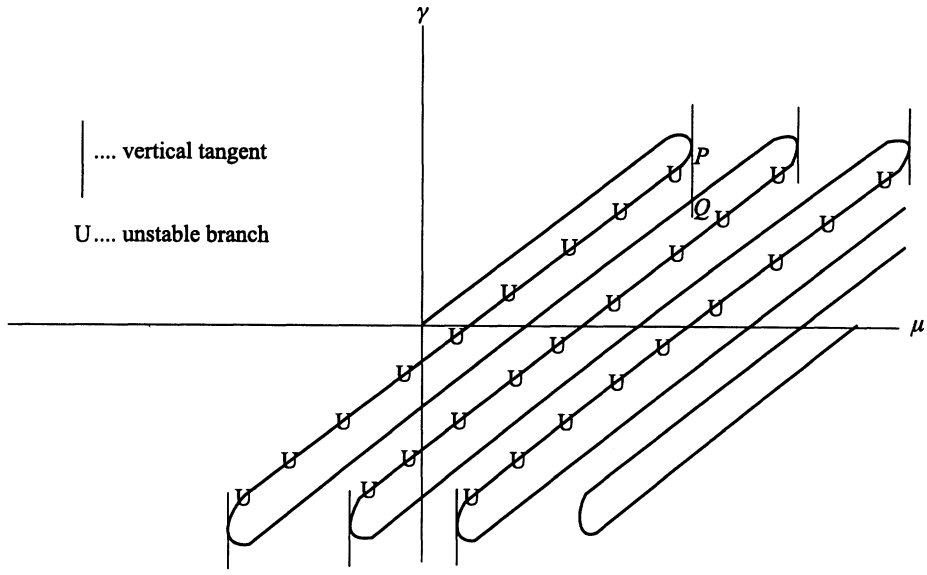

Fig. 5. Locus of stationary pairs under prescribed macroshear.

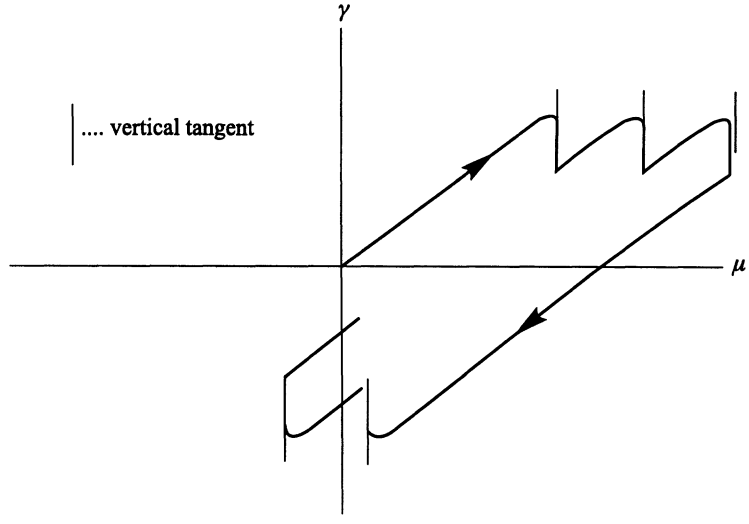

Fig. 6. Hysteretic response under prescribed macroshear.

Downloaded from http://mms.sagepub.com at SIMON FRASER LIBRARY on November 11, 2008

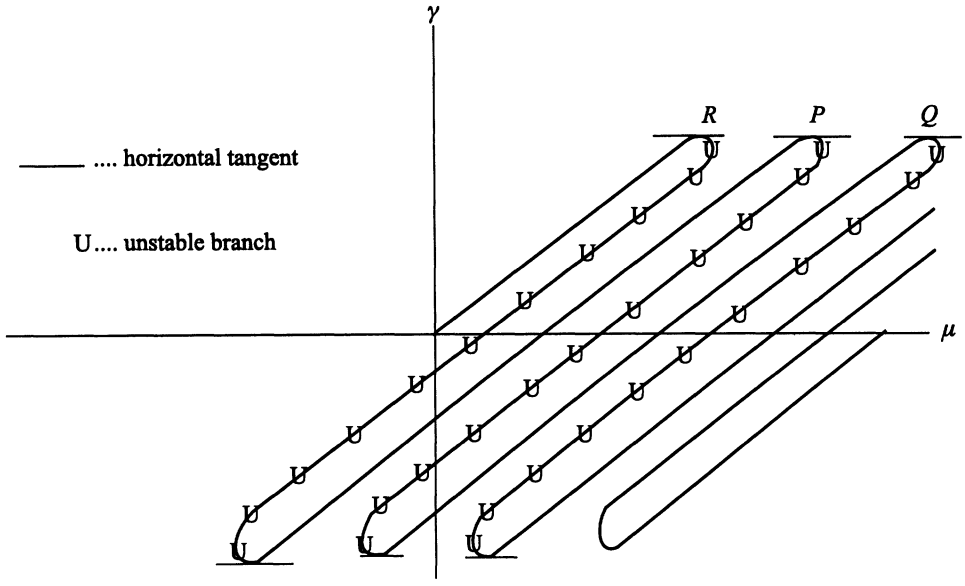

Fig. 7. Locus of stationary points under prescribed shear stress.

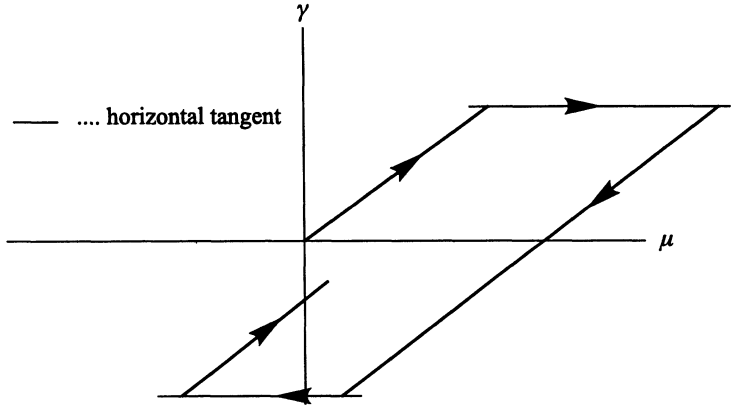

Fig. 8. Hysteretic response under prescribed shear stress.

Downloaded from http://mms.sagepub.com at SIMON FRASER LIBRARY on November 11, 2008

situation reverses, and horizontal jumps to the left decrease the total energy $\mathcal{E}$. For a shearing process in which the shear stress σ first is increased, then decreased, and again is increased, the hysteresis loop shown in Figure 8 is consistent with the requirements that the pair (μ, γ) remain on a stable branch of the locus of stationary pairs, and, when the pair jumps from one stable branch to another, the total energy decreases. The examples illustrated in Figures 6 and 8 show that the class of two-level shears together with the form of the free energy in (24) lead to collections of equilibrium states that are compatible with hysteresis in processes for which the macroscopic shear is controlled and in processes for which the shear stress is controlled.

4.2. Yielding and Dissipation Associated with Two-Level Shears

Before describing in Subsection 4.3 specific kinds of materials that exhibit such hysteretic response, we identify in these processes the counterparts of yielding, reversible loading and unloading, and dissipation.

For processes in Case 2, where the shear stress is specified, relation (31) and the fact that ψ' is a bounded function imply that the magnitude of the shear stress cannot exceed the maximum value of $|\psi'|$. Processes that attain and maintain that value may cause the shear due to microslip $\mu - \gamma$ to jump by an amount equal to an integral multiple of the period p of the microslip energy ψ. This jump arises when the stationary pair (μ, γ) reaches the end of a stable branch of the locus of stationary pairs and jumps horizontally to another branch, while decreasing the total energy. We identify this behavior as yielding of the material due to material instabilities at the micro level. Because the free energy is constant in the horizontal jumps, we may identify the work $\sigma[\mu - \gamma] = \sigma[\mu]$ as the dissipation arising due to the microinstability, where, as before, $[\cdot]$ denotes the jump in a given quantity. As noted above, σ and the jump $[\mu]$ have the same sign; consequently, the dissipation is positive, in agreement with thermodynamics. It is interesting to note that yielding is not the only circumstance in which microslip occurs. In fact, relation (31) and the fact that $\psi'(0) = 0$ show that, when the shear stress σ is nonzero, then so is the shear due to microslip $\mu - \gamma$. Hence, nonzero shear stresses below the yield value $\sigma_y := \max|\psi'|$ also cause microslip. However, the microslip below the yield value occurs without dissipation, in the sense that the work done and the accompanying change in free energy $\mathcal{I}$ are equal. In fact, by (31), (32), and (24), we may write

$$\begin{aligned} \int \sigma d\mu &= \int \psi'(\mu - \gamma) d\mu + \left(\varphi'(\gamma) - \psi'(\mu - \gamma)\right) d\gamma \\ &= \int \frac{\partial \mathcal{I}}{\partial \mu} d\mu + \frac{\partial \mathcal{I}}{\partial \gamma} d\gamma = \Delta \mathcal{I}. \end{aligned} \tag{35}$$

Thus, whereas the microslip at yield occurs in the form of a jump in $\mu - \gamma$ and is dissipative, the microslip below yield occurs as a continuous variation in $\mu - \gamma$ without dissipation.

For processes in Case 1, where the macroshear μ is specified, the magnitude $|\gamma|$ of the shear without microslip is subject to a bound by virtue of relation (26) and the assumptions (i) and (ii) on φ and ψ. However, $|\gamma|$ must decrease subsequent to the attainment of that

Downloaded from http://mms.sagepub.com at SIMON FRASER LIBRARY on November 11, 2008

bound before dissipative behavior occurs. In fact, it is only when relation (29) is satisfied that an unstable branch of the locus of stationary pairs is encountered. At such a point, $|\gamma|$ jumps to a smaller value, μ remains constant, and the free energy decreases without work being done. Thus, the shear due to microslip experiences a jump that is accompanied by dissipation, and the material yields at a fixed value of the macroshear and at a value of $|\gamma|$ below its maximum. We again identify this behavior as a yielding due to microinstabilities; the accompanying dissipation is simply the magnitude of the change in free energy associated with the jump in γ. At stages of a process under controlled macroshear, microslip occurs as long as γ is nonzero, just as is the case in a process under controlled, nonzero shear stress. If we identify the shear stress under controlled macroshear as the quantity $\varphi'(\gamma)$, then the calculation in (35) shows that, just as for the case of controlled shear stress, microslip in the absence of microinstabilities occurs without dissipation. An interpretation of yielding as a material instability was given in the 1930s by Nakanishi [13, pp. 3, 127]. The possibility that microscopic instabilities are the source of yielding and hysteresis was studied in the doctoral dissertation of Grolig [14], written under the supervision of P. Haupt.

4.3. Two-Level Shears and Slip Mechanisms in Single Crystals

The cases considered in Subsections 4.1 and 4.2 show that the collection of equilibrium pairs within the class of two-level shears is rich enough to capture simply and directly features of yielding, hysteresis, and dissipation reminiscent of observed phenomenological properties of metals. In this subsection, we describe in more detail connections between two-level shears and the behavior of specific kinds of materials. We have in mind the use of two-level shears to model the shearing of a piece of a single crystal that contains a large number of parallel slip bands, whose thickness is each about 100 atomic units [15]. For the sequence $n \longmapsto (\kappa_n, f_n)$ of simple deformations in (21), the disarrangement sites κ_n form a collection of equally spaced parallel planes, and we identify each plane with a slip band. By (21), the jump in transplacement $[f_n]$ across each slip band is $(\mu - \gamma)/n$, and the vertical separation of neighboring slip bands is $1/n$, so that the relation

$$\mu - \gamma = \frac{(\mu - \gamma)/n}{1/n} \tag{36}$$

identifies the shear due to microslip $\mu - \gamma$ as the (limiting) ratio of horizontal slip to vertical spacing of the array of slip bands. This formula for our measure $\mu - \gamma$ of deformation due to microslip is consistent with the definition of shear strain due to slip given by Taylor [16] in his studies of single crystals. Note that if the horizontal slip across a given slip band is one atomic unit and the separation of slip bands is 10,000 atomic units (as suggested in the discussion by Hill [15, pp. 4–7]), then we may conclude that the shear due to microslip is 10^{-4}. A horizontal slip of one atomic unit has particular significance for the free energy $\mathcal{I}$, because such a slip translates the two halves of the crystal determined by the slip band relative to one another while restoring the original atomic configuration of the two halves. Therefore, if we interpret the term $\psi(\mu - \gamma)$ in (24) as the energy associated with microslip, we are led to our earlier assumption in (ii) that ψ is periodic. Moreover, in the case where slip bands are separated by 10,000 atomic units, $\mu - \gamma$ changes by 10^{-4} in a slip of one atomic unit, and we

Downloaded from http://mms.sagepub.com at SIMON FRASER LIBRARY on November 11, 2008

are led to set the period p of ψ equal to 10^{-4}. Because γ is the shear without microslip, we interpret the term $\varphi(\gamma)$ in (24) as the energy due to distortion of the crystalline lattice without the presence of slip.

It is instructive at this point to choose specific functions φ and ψ consistent with assumptions (i) and (ii). For example, we take

$$\begin{aligned} \varphi(\gamma) &:= \frac{1}{2}k\gamma^2 \\ \psi(\mu-\gamma) &:= \frac{\Psi_0}{2\pi \times 10^4}\{1-\cos(2\pi \times 10^4(\mu-\gamma))\}, \end{aligned} \tag{37}$$

with the positive numbers Ψ_0 and k to be further restricted below. (Recall from the discussion at the end of Section 3 that the choice $W(A) = \frac{k}{2}|A-\mathbb{I}|^2$ of initial bulk energy density ensures that the decomposition (23), with lattice energy density given by $(37)_1$, is a consequence of the representation (22).) The stationarity condition (32) then becomes

$$\gamma = \frac{\Psi_0}{k}\sin(2\pi \times 10^4(\mu-\gamma)), \tag{38}$$

and the condition (34) for microinstability under prescribed shear stress reads

$$\cos(2\pi \times 10^4(\mu-\gamma)) = 0, \tag{39}$$

an equation whose smallest positive solution is

$$\mu-\gamma = \frac{1}{4}\times 10^{-4}. \tag{40}$$

The discussion in [15] also suggests that the amount of strain at which dissipation first arises is also 10^{-4}, and we take this to mean that microinstability first occurs when μ attains that value. Thus, at the onset of microinstability, we may conclude from (40) that γ equals $\frac{3}{4}\times 10^{-4}$ and, from (38), that $\frac{\Psi_0}{k}$ equals $\frac{3}{4}\times 10^{-4}$. Therefore, the implicit relation (38) between γ and μ becomes

$$\gamma = \frac{3}{4}\times 10^{-4}\sin(2\pi \times 10^4(\mu-\gamma)) \tag{41}$$

(see Figure 9), and, indeed, with this value of the ratio $\frac{\Psi_0}{k}$, the functions φ and ψ satisfy the conditions (i) and (ii) in Section 4.1. Moreover, (37) implies the relations

$$\varphi_{yield} = \frac{9k}{32}\times 10^{-8}$$

Downloaded from http://mms.sagepub.com at SIMON FRASER LIBRARY on November 11, 2008

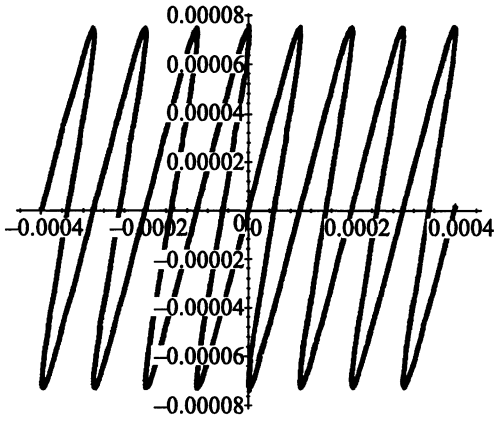

Fig. 9. γ versus μ from equation (41).

$$\psi_{yield} = \frac{3k}{8\pi} \times 10^{-8}, \tag{42}$$

where the subscript "yield" indicates the value at the onset of microinstability under prescribed shear stress. We conclude that the ratio of the lattice energy to the microslip energy at yield is given by

$$\frac{\varphi_{yield}}{\psi_{yield}} = \frac{3\pi}{4}. \tag{43}$$

On the other hand, the limit as the macroshear μ tends to zero of the ratio at equilibrium of lattice energy to microslip energy is readily calculated and has the value

$$\left(\frac{\varphi}{\psi}\right)_0 := \lim_{\mu \to 0} \frac{\varphi(\gamma)}{\psi(\mu - \gamma)} = \frac{3\pi}{2}. \tag{44}$$

Consequently, the specific choice (37) of φ and ψ implies that the ratio φ/ψ is halved in proceeding from the initiation of shear to the onset of microinstability.

5. AN APPLICATION TO FRACTURE MECHANICS

5.1. Equilibrium Configurations of a Bar

Let E be one-dimensional, let $l > 0$, and assume that a bar in its reference configuration occupies the interval $(0, l)$. To emphasize the features of our analysis of fracture that differ from the applications in Section 4, we focus our attention on the contributions to the energy of the bar due to macroscopic deformation and to macroscopic disarrangements (fracture), leaving out the effects of microscopic disarrangements. Accordingly, we consider in this section only simple deformations (κ, f) from $(0, l)$. The definition of a simple deformation

Downloaded from http://mms.sagepub.com at SIMON FRASER LIBRARY on November 11, 2008

in Section 2.1 applied to the present one-dimensional context tells us that κ is a finite subset of $(0,l)$; f is an injective, bounded, piecewise C^1 function whose jump set $\Gamma(f)$ is a subset of κ; and ∇f is a bounded, piecewise continuous function with a strictly positive lower bound. We rule out the drastic case in which pieces of the bar can be interchanged after fracture by restricting our attention further to the case where f is strictly increasing, so that the jump $[f](z)$ is positive for every $z \in \Gamma(f)$. In this context, we take the energy of a simple deformation (κ, f) to be

$$E(\kappa, f) = \int_0^l W(\nabla f(x))dx + \sum_{z\in\kappa} \Theta([f](z)). \tag{45}$$

We assume that W is strictly convex, twice continuously differentiable with second derivative bounded below by a positive constant, and $W(1) = W'(1) = 0$. We assume further that the interfacial energy density $\Theta : [0,\infty) \to \mathbb{R}$ satisfies the hypotheses (H2) and (H3) made in Section 3, with the unit vector ν replaced here by the number one. It follows that Θ is nonnegative with $\Theta(0) = 0$ and that Θ cannot be strictly convex. In view of the intended applications to fracture, it is assumed on the interval $(0,\infty)$ that Θ is twice continuously differentiable with strictly negative second derivative and bounded first derivative, so that Θ is strictly concave, Θ' is strictly decreasing, and $0 < \Theta'(0+) < \infty$. We note that the condition $\Theta(0) = 0$ permits us to replace κ by $\Gamma(f)$ as the range of summation in relation (45), since at the points in $\kappa \setminus \Gamma(f)$ the jump in f vanishes, and therefore the corresponding energy does not contribute to the sum. Accordingly, we write $\Gamma(f)$ in place of κ and f in place of (κ, f) in what follows.

Suppose now that the bar is constrained by means of a hard device; that is, the length $\beta l = f(l-) - f(0+)$ after a simple deformation f is specified. By formula (3.16) of [1],

$$\int_0^l \nabla f(x)dx + \sum_{z\in\Gamma(f)} [f](z) = \beta l. \tag{46}$$

The total energy of the bar then coincides with the energy in (45), and the condition that the bar be in equilibrium implies the vanishing of the first variation

$$\delta E(f;\nu) = \int_0^l W'(\nabla f(x))\nabla\nu(x)dx + \sum_{z\in\Gamma(f)} \Theta'([f](z))[\nu](z) \tag{47}$$

for all variations ν such that

a. $f+\nu$ is a simple deformation from $(0,l)$ with $\Gamma(f+\nu) \subset \Gamma(f)$
b. condition (46) is satisfied with f replaced by $f+\nu$, or, equivalently,

$$\int_0^l \nabla\nu(x)dx + \sum_{z\in\Gamma(f)} [\nu](z) = 0. \tag{48}$$

Downloaded from http://mms.sagepub.com at SIMON FRASER LIBRARY on November 11, 2008

Variations v such that $\Gamma(f+v)\backslash\Gamma(f) \neq \emptyset$ require a different argument and will be examined in Section 5.2. Let $x_1 < x_2$ in $(0,l)\backslash\Gamma(f)$ and ε in $(0, \min\{x_2-x_1, x_1, l-x_2\})$ be given. Choose $v_{\varepsilon,d}$ to be the continuous, piecewise C^1 mapping from $(0,l)$ into $\mathbb{R}$ such that $v_{\varepsilon,d}(0+) = 0$ and

$$\nabla v_{\varepsilon,d}(x) = \begin{cases} d & \text{if} \quad x \in (x_1-\varepsilon, x_1+\varepsilon) \\ -d & \text{if} \quad x \in (x_2-\varepsilon, x_2+\varepsilon) \\ 0 & \text{otherwise,} \end{cases} \tag{49}$$

with

$$d := \inf\{\nabla f(x) \,:\, x \in (0,l)\backslash\Gamma(f)\}/2 > 0. \tag{50}$$

Thus, $f+v_{\varepsilon,d}$ agrees with g on $(0, x_1-\varepsilon]$ and on $[x_2+\varepsilon, l)$, increases more rapidly than f on $(x_1-\varepsilon, x_1+\varepsilon)$, more slowly than f on $(x_2-\varepsilon, x_2+\varepsilon)$, and at the same rate elsewhere. By the choice of d, $f+v_{\varepsilon,d}$ is bounded, piecewise C^1 with derivative having a strictly positive lower bound, so that $f+v$ also is a simple deformation. It is clear that $v_{\varepsilon,d}$ satisfies the condition (48), and the vanishing of the first variation (47) yields

$$\int_{-\varepsilon}^{\varepsilon} \Big(W'(\nabla f(x_1+\xi)) - W'(\nabla f(x_2+\xi)) \Big)\, d\xi = 0. \tag{51}$$

Because x_1 and x_2 are points of continuity of ∇f, and because W' is continuous and $\varepsilon \in (0, \min\{x_2-x_1, x_1, l-x_2\})$ is arbitrary, we conclude that $W'(\nabla f(x_1)) - W'(\nabla f(x_2)) = 0$. The strict convexity of W then tells us that $\nabla f(x_2) = \nabla f(x_1)$, and because x_1 and x_2 are arbitrary points in $(0,l)\backslash\Gamma(f)$, we conclude that a necessary condition for equilibrium of the bar in the configuration determined by f is that ∇f be constant on $(0,l)\backslash\Gamma(f)$. Therefore, (47) becomes

$$\delta E(f;v) = S\int_0^l \nabla v(x)dx + \sum_{z\in\Gamma(f)} \Theta'([f](z))[v](z), \tag{52}$$

where $S := W'(\nabla f) \geq 0$ is called the equilibrium stress. In view of the constraint (48), the vanishing of the first variation and (52) imply

$$\sum_{z\in\Gamma(f)} (\Theta'([f](z)) - S)[v](z) = 0. \tag{53}$$

Let $z_1 \in \Gamma(f)$ and recall that the jump $[f](z_1)$ is nonnegative. Therefore, for each $A \in (0,d)$, the function $f+v_A$, with

$$v_A(x) = \begin{cases} -Ax & \text{for} \quad x \in (0, z_1) \\ -Ax + lA & \text{for} \quad x \in [z_1, l) \end{cases} \tag{54}$$

is a simple deformation satisfying the constraint (48) and with jump $Al + [f](z_1)$ at z_1. Consequently, relation (53) applied to the variation v_A yields the condition

Downloaded from http://mms.sagepub.com at SIMON FRASER LIBRARY on November 11, 2008

$$\Theta'([f](z_1)) = S \tag{55}$$

for all $z_1 \in \Gamma(f)$. To summarize, necessary conditions for equilibrium of the bar under the simple deformation f are constancy of ∇f on $(0,l)\backslash\Gamma(f)$ and of $[f]$ on $\Gamma(f)$, as well as the relation

$$\Theta'([f]) = W'(\nabla f). \tag{56}$$

The relations (46) and (56) then imply that, if the bar is in equilibrium with $\beta < 1$, then $\Gamma(f)$ is empty, so that equilibrium under compression entails no fracture. Indeed, if $\beta < 1$ and $\Gamma(f) \neq \emptyset$, since $[f] > 0$, we would have $\Theta'([f]) = W'(\nabla f) > 0$, so that $\nabla f > 1$. On the other hand, we would also have

$$l > \beta l = \int_0^l \nabla f dx + \sum_{z\in\Gamma(f)} [f](z) > \int_0^l \nabla f dx > l,$$

a contradiction. We note, finally, that the monotonicity of Θ' on $[0,\infty)$ tells us that we may solve the relation (56) for $[f]$ as a function of ∇f when the jump set $\Gamma(f)$ is not empty:

$$[f] = h(\nabla f), \tag{57}$$

where the decreasing, positive-valued, differentiable function h is the inverse of Θ' composed with W':

$$h = \Theta'^{-1} \circ W'. \tag{58}$$

For future reference, we note that

$$h^{-1}(0+) > 1. \tag{59}$$

Indeed, $\Theta'(0+) > 0$ by assumption. Then, $W'^{-1}(\Theta'(0+)) > W'^{-1}(0)$, since W'^{-1} is monotonic, and the two members of this inequality are equal to $h^{-1}(0+)$ and 1, respectively.

5.2. Metastable Configurations

Among the equilibrium configurations of the bar, we are interested in those that are metastable, that is, are local minimizers of the energy in a sense to be made precise below. Taking into account the constancy of ∇f and the relation (57), we have the necessary condition for metastability:

$$\delta\,\delta\, E(f)(v,v) = W''(\nabla f)\int_0^l \nabla v(x)^2 dx + \Theta''(h(\nabla f)) \sum_{z\in\Gamma(f)} [v]^2(z) \geq 0 \tag{60}$$

Downloaded from http://mms.sagepub.com at SIMON FRASER LIBRARY on November 11, 2008

for all variations v satisfying (48) and such that $f+v$ is a simple deformation with $\Gamma(f+v) \subset \Gamma(f)$. By choosing a continuous variation, we conclude immediately that $W''(\nabla f)$ must be nonnegative, as assumed at the beginning of Section 5.1. A further necessary condition for metastability is obtained from (60) with the choice v_A given in (54); namely,

$$lW''(\nabla f)A^2 + \Theta''(h(\nabla f))l^2A^2 \geq 0,$$

so that

$$W''(\nabla f) + l\Theta''(h(\nabla f)) \geq 0. \tag{61}$$

Finally, for points $z_1 < z_2$ in $\Gamma(f)$ and for each ζ with $|\zeta| \leq \min\{[f](z_1), [f](z_2)\}$, we may choose the variation $v_{2,\zeta}$ defined by

$$v_{2,\zeta}(x) = \begin{cases} 0 & \text{for } x \in (0, z_1) \\ \zeta & \text{for } x \in (z_1, z_2) \\ 0 & \text{for } x \in (z_2, l), \end{cases} \tag{62}$$

and obtain from (60) the necessary condition

$$\Theta''(h(\nabla f)) \geq 0,$$

which contradicts the assumed negativity of Θ''. In other words, simple deformations with more than one jump point cannot be metastable.

Returning momentarily to first variations of the energy, we consider now the case of a variation v for which $\Gamma(f+v)\backslash\Gamma(f) \neq \emptyset$. For example, choose $z_1 \notin \Gamma(f)$, let $\delta \in [0, d)$ be given with d defined in (50), and choose a variation v as in (54) with $A := \delta/2$ to obtain the energy

$$E(f+v) = lW\left(\nabla g - \frac{\delta}{2}\right) + \sum_{z \in \Gamma(f)} \Theta([f](z)) + \Theta(l\delta/2) \tag{63}$$

for a simple deformation that perturbs f by adding one crack of magnitude $l\delta/2$ and reducing the stretch in the bar elsewhere so as to maintain the prescribed length βl. A necessary condition for equilibrium is that the right-hand derivative of the right-hand side of (63) at $\delta = 0$ be nonnegative. This condition, along with the relation (56), implies

$$\Theta'(0+) \geq W'(\nabla f) = S. \tag{64}$$

In other words, in equilibrium, the stress is no greater than the positive number $\Theta'(0+)$.

We turn now to sufficient conditions for obtaining a local minimizer of the energy. It can be proved [21] that if we define the distance between two simple deformations f and $\bar{f}$ by

$$d(f,\bar{f}) := \sup_{x \in (0,l)\backslash(\Gamma(f) \cup \Gamma(\bar{f}))} (|f(x) - \bar{f}(x)| + |\nabla f(x) - \nabla \bar{f}(x)|),$$

Downloaded from http://mms.sagepub.com at SIMON FRASER LIBRARY on November 11, 2008

then we obtain the following sufficient conditions for a simple deformation f to correspond to a metastable configuration of the bar:

A. ∇f is constant
B. f has at most one jump point
C. Relation (56) is satisfied if f does have a jump point
D. Relation (64) is satisfied with strict inequality
E. Relation (61) is satisfied with strict inequality.

These sufficient conditions differ from the necessary conditions obtained above only by the fact that inequalities (61) in (E) and (64) in (D) must now be strict. Note also that the choice of distance d is consistent with the notion of convergence given in formulas (6) and (7) in Section 2.1.

We consider the form that relation (46) assumes for metastable configurations:

$$\beta = \begin{cases} \nabla f & \text{when } f \text{ has no jumps} \\ \nabla f + \frac{h(\nabla f)}{l} & \text{when } f \text{ has one jump,} \end{cases} \tag{65}$$

where h is the decreasing, differentiable function in (58). The formula for the energy E in (45) becomes

$$E(f) = \begin{cases} W(\nabla f)\, l & \text{when } f \text{ has no jumps} \\ W(\nabla f)\, l + \Theta(h(\nabla f)) & \text{when } f \text{ has one jump.} \end{cases} \tag{66}$$

We consider from now on the case $\beta \geq 1$ in which the bar is extended beyond its natural length l. Our goal is to study the relations between β and ∇f at metastable configurations. For configurations in which g has no jumps, because W' is invertible, the inequality (64) can be rewritten in the form

$$\nabla f \leq W'^{-1}(\Theta'(0+)). \tag{67}$$

We also have from (65) that $\nabla f \geq 1$, and we conclude that

$$1 \leq \nabla f \leq h^{-1}(0+).$$

Hence, for simple deformations in which f has no jump and $\beta \geq 1$, the deformation gradient $\nabla f = \beta$ is bounded above by $h^{-1}(0+)$. Moreover, relation (57) tells us that if f has a jump, then ∇f must be in the range of h^{-1} and we may conclude that extension with a jump can occur only if

$$\inf Rng(h^{-1}) \leq \nabla f < \beta \quad \text{and} \quad \nabla f \leq h^{-1}(0+). \tag{68}$$

In particular, if $\inf \Theta'$ is positive, then $\inf Rng(h^{-1}) > 1$, and the bar extends from length l up to length $\inf Rng(h^{-1})l$ without fracture. When ∇f is in the interval $(\inf Rng(h^{-1}), h^{-1}(0+)]$, both of the relations between ∇f and β in (65) must be considered. Differentiation of the second relation in (65) with respect to ∇f, together with (56), (57), condition (E), and the negativity of Θ'', yields

Downloaded from http://mms.sagepub.com at SIMON FRASER LIBRARY on November 11, 2008

$$\frac{d\beta}{d\nabla f} = 1 + \frac{W''(\nabla f)}{l\Theta''(h(\nabla f))} = \frac{W''(\nabla f) + l\Theta''(h(\nabla f))}{l\Theta''(h(\nabla f))} < 0 \tag{69}$$

for metastable configurations with one crack. Thus, the metastable portion of the locus in the $\nabla f - \beta$ plane representing equilibrium configurations with one crack

$$\mathcal{L}_c := \left\{ \left(\nabla f, \nabla f + \frac{h(\nabla f)}{l} \right) \,:\, \nabla f \in (\inf Rng(h^{-1}), h^{-1}(0+)) \right\} \tag{70}$$

consists only of branches on which the extension β is a decreasing function of ∇f. Relation (65) describes not only the locus $\mathcal{L}_c$ but also the locus

$$\mathcal{L}_\backslash := \{ (\nabla f, \nabla f) \,:\, \nabla f \in [1, h^{-1}(0+)] \} \tag{71}$$

of equilibrium configurations without a crack. According to the sufficient conditions for metastability listed above, all of the points on $\mathcal{L}_\backslash$ are metastable.

Various possibilities for the geometry of the graph of the relation (65) arise depending on the length l of the undeformed bar and the functions W and Θ. For definiteness, we consider here only the case in which $\inf \Theta'$ is positive. In this case, there are two possibilities, depending on whether l is greater than or smaller than the critical length

$$l_c := -\frac{W''(\beta_P)}{\Theta''(\beta_P)}, \tag{72}$$

with $\beta_P := h^{-1}(0+)$. The first possibility, $l > l_c$, corresponds to the case in which both the unstable and the stable portions of $\mathcal{L}_c$ are nonempty, as illustrated in Figure 10. We note that the two loci $\mathcal{L}_\backslash$ and $\mathcal{L}_c$ meet at the point $P = (\beta_P, \beta_P)$. Moreover, the horizontal line through the low point R on $\mathcal{L}_c$ and the horizontal line through P determine an interval (β_R, β_P) of extensions β for each of which there are three choices of ∇f such that the point $(\nabla f, \beta)$ represents an equilibrium configuration of the bar. We identify the three corresponding branches of equilibrium pairs in Figure 10 from point R to Q, from R to P, and from S to P by the symbols $\mathcal{L}_{RQ}$, $\mathcal{L}_{RP}$, and $\mathcal{L}_{SP}$, respectively, and we note that $\mathcal{L}_{RP}$ is the unstable branch, that $\mathcal{L}_{QR} \cup \mathcal{L}_{RP} \subset \mathcal{L}_c$, and that $\mathcal{L}_{SP} \subset \mathcal{L}_\backslash$. On each of the branches $\mathcal{L}_{RQ}$ and $\mathcal{L}_{RP}$ of $\mathcal{L}_c$ and on the single branch $\mathcal{L}_{SP}$ of $\mathcal{L}_\backslash$, we may use (65) to express ∇f as a function of β, $\nabla f = \mathcal{G}(\beta) \leq \beta$ for β in the interval (β_R, β_P) shown in Figure 10. For each of these three branches, we can express the energy as a function of β,

$$\left.\begin{aligned} E_{RQ}(\beta) &= lW(\mathcal{G}_{RQ}(\beta)) + \Theta(h(\mathcal{G}_{RQ}(\beta))), \\ E_{RP}(\beta) &= lW(\mathcal{G}_{RP}(\beta)) + \Theta(h(\mathcal{G}_{RP}(\beta))), \\ E_{SP}(\beta) &= lW(\beta) \end{aligned}\right\}, \tag{73}$$

and we wish to compare these energies at each β in the interval (β_R, β_P). We note first that

$$E_{RQ}(\beta_R) = E_{RP}(\beta_R) \qquad \text{and} \qquad E_{RP}(\beta_P) = E_{SP}(\beta_P), \tag{74}$$

Downloaded from http://mms.sagepub.com at SIMON FRASER LIBRARY on November 11, 2008

since $\mathcal{L}_{RQ}$ and $\mathcal{L}_{RP}$ intersect at the point R and $\mathcal{L}_{RP}$ and $\mathcal{L}_{SP}$ intersect at the point P. Next, we compute the derivative of $E_{RQ} - E_{RP}$. Recalling from (65) that $h(\mathcal{G}(\beta)) = l(\beta - \mathcal{G}(\beta))$, we have

$$\frac{d}{d\beta}h(\mathcal{G}(\beta)) = l(1 - \frac{d}{d\beta}\mathcal{G}(\beta)), \tag{75}$$

and therefore, by (73), we obtain the formula

$$\begin{aligned}\frac{d}{d\beta}(E_{RQ}(\beta) - E_{RP}(\beta)) &= lW'(\mathcal{G}_{RQ}(\beta))\frac{d}{d\beta}\mathcal{G}_{RQ}(\beta)\\ &+ \Theta'(h(\mathcal{G}_{RQ}(\beta)))l\left(1 - \frac{d}{d\beta}\mathcal{G}_{RQ}(\beta)\right)\\ &- lW'(\mathcal{G}_{RP}(\beta))\frac{d}{d\beta}\mathcal{G}_{RP}(\beta)\\ &- \Theta'(h(\mathcal{G}_{RP}(\beta)))l\left(1 - \frac{d}{d\beta}\mathcal{G}_{RP}(\beta)\right).\end{aligned}$$

By employing (56) in the form $W'(\mathcal{G}(\beta)) = \Theta'(h(\mathcal{G}(\beta)))$, we can reduce this relation to the simple form

$$\frac{d}{d\beta}(E_{RQ}(\beta) - E_{RP}(\beta)) = lW'(\mathcal{G}_{RQ}(\beta)) - lW'(\mathcal{G}_{RP}(\beta)). \tag{76}$$

Because W is a smooth, strictly convex function, its derivative W' is strictly increasing; moreover, the definitions of the branches $\mathcal{L}_{RQ}$ and $\mathcal{L}_{RP}$ imply the relation $\mathcal{G}_{RQ}(\beta) < \mathcal{G}_{RP}(\beta)$ for all β in the interval (β_R, β_P). We conclude that the right-hand side of (76) is negative and, therefore, that the difference $E_{RQ} - E_{RP}$ is strictly decreasing on $[\beta_R, \beta_P]$. However, by $(74)_1$, this difference vanishes at β_R, so that

$$E_{RQ}(\beta) < E_{RP}(\beta) \tag{77}$$

for all β in the interval $(\beta_R, \beta_P]$. Similarly, the computation of the derivative of $E_{RP} - E_{SP}$ yields in place of (76) the relation

$$\frac{d}{d\beta}(E_{RP}(\beta) - E_{SP}(\beta)) = lW'(\mathcal{G}_{RP}(\beta)) - lW'(\mathcal{G}_{SP}(\beta)),$$

from which we conclude that $E_{RP} - E_{SP}$ also is strictly decreasing on $[\beta_R, \beta_P]$. Because this difference vanishes at β_P by $(74)_2$, we have

$$E_{SP}(\beta) < E_{RP}(\beta) \tag{78}$$

Downloaded from http://mms.sagepub.com at SIMON FRASER LIBRARY on November 11, 2008

for all β in the interval $[\beta_R, \beta_P)$. From the fact that both $E_{RQ} - E_{RP}$ and $E_{RP} - E_{SP}$ are strictly decreasing, it follows that the difference $E_{RQ} - E_{SP} = (E_{RQ} - E_{RP}) + (E_{RP} - E_{SP})$ is strictly decreasing. Moreover, relations (74), (77), and (78) tell us that

$$\begin{aligned} E_{RQ}(\beta_R) - E_{SP}(\beta_R) &= E_{RP}(\beta_R) - E_{SP}(\beta_R) > 0 \\ E_{RQ}(\beta_P) - E_{SP}(\beta_P) &= E_{RQ}(\beta_P) - E_{RP}(\beta_P) < 0, \end{aligned}$$

and the continuity and monotonicity of $E_{RQ} - E_{SP}$ then yield the following conclusion: there exists exactly one extension β_F in the interval (β_R, β_P) such that (a) $E_{RQ}(\beta) > E_{SP}(\beta)$ for all $\beta \in [\beta_R, \beta_F)$ and (b) $E_{RQ}(\beta) < E_{SP}(\beta)$ for all $\beta \in (\beta_F, \beta_P]$. As the extension β increases from β_R to β_P, when $\beta = \beta_F$ it becomes energetically favorable for a metastable equilibrium pair $(\mathcal{G}_{SP}(\beta), \beta)$ on the locus $\mathcal{L}_{SP}$ to jump to a metastable equilibrium pair $(\mathcal{G}_{RQ}(\beta), \beta)$ on the locus $\mathcal{L}_{RQ}$. In passing through the extension β_F, the deformation gradient ∇f decreases discontinuously from β_F to $\mathcal{G}_{RQ}(\beta_F)$ due to the appearance of a positive jump

$$h(\mathcal{G}_{RQ}(\beta)) = l(\beta_F - \mathcal{G}_{RQ}(\beta_F)) \tag{79}$$

in the transplacement. This sudden appearance of an opened crack is referred to as brittle fracture, as distinguished from the ductile fracture to be described below, and the concentration of deformation at the site of the crack, with consequent decrease in the deformation gradient away from the crack, is an instance of strain localization in the sense described, for example, in [20].

The second possibility, $l < l_c$, is illustrated in Figure 11. In this case, the locus $\mathcal{L}_c$ consists entirely of metastable pairs. Because the two loci $\mathcal{L}_\setminus$ and $\mathcal{L}_c$ must meet at the point P, each horizontal line $\beta = const.$ meets the equilibrium locus $\mathcal{L}_\setminus \cup \mathcal{L}_c$ in exactly one point. Thus, as the extension β increases from its minimum value 1 to the value β_P, metastable equilibrium configurations of the bar follow the locus $\mathcal{L}_\setminus$, and as β increases beyond β_P, the configurations follow the locus $\mathcal{L}_c$, without the appearance, as was the case for brittle fracture, of a sudden lowering of the deformation gradient ∇f at the transition point P. Thus, in the present case, a crack appears at the extension β_P and opens gradually as β increases above this value. A corresponding gradual lowering of the deformation gradient ∇f accompanies the opening of the crack, as is shown in Figure 11. This situation is described by saying that ductile fracture occurs as the bar passes through the equilibrium configuration corresponding to the pair P. The preceding analysis enables us to deduce deformation elongation curves, ∇f versus β, for the bar. In view of the identification of the equilibrium stress S as the derivative $W'(\nabla g)$ of the bulk energy W, and by the assumed convexity of W, there is a one-to-one correspondence between S and ∇f, $S = W'(\nabla f)$, which makes it possible to obtain stress elongation curves, S versus β, from the deformation elongation relations in Figures 10 and 11. In fact, there are two types of stress elongation curves for given energy densities W and Θ, depending on whether the length of the bar is greater than or less than the critical length l_c. These two types of curves correspond to brittle and ductile fracture, respectively. In brittle fracture, the stress increases with β to the value $W'(\beta_F)$, whereupon there is a

Downloaded from http://mms.sagepub.com at SIMON FRASER LIBRARY on November 11, 2008

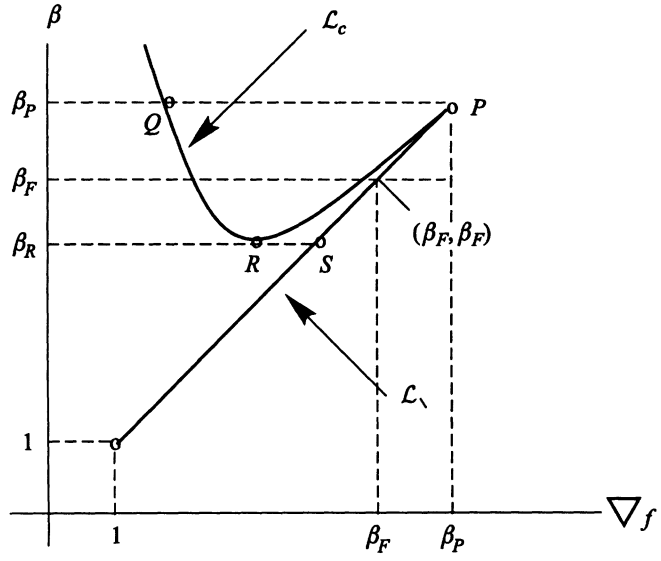

Fig. 10. Equilibrium loci for brittle fracture.

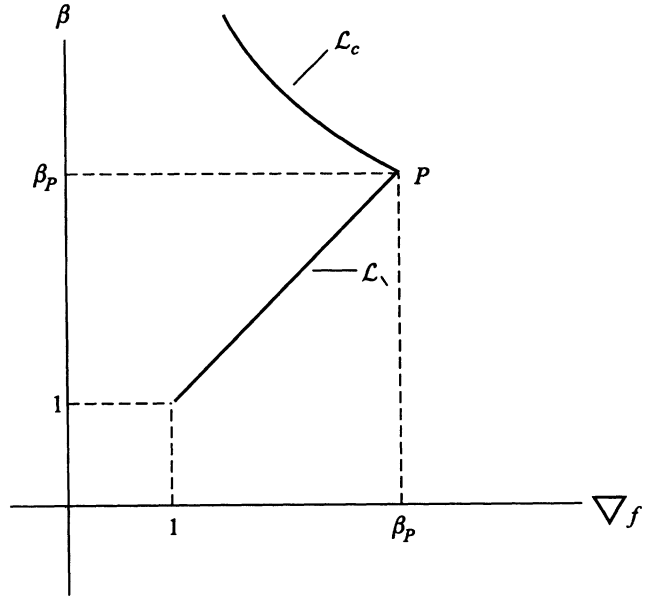

Fig. 11. Equilibrium locus for ductile fracture.

Downloaded from http://mms.sagepub.com at SIMON FRASER LIBRARY on November 11, 2008

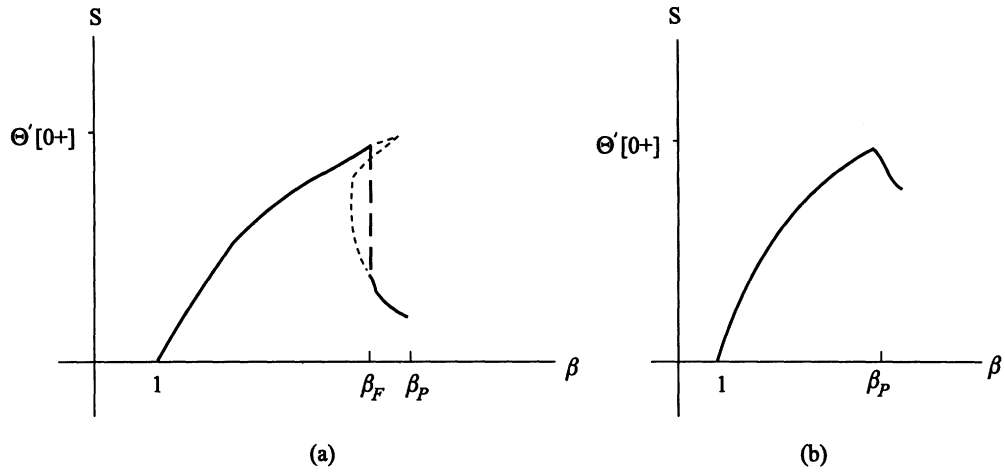

Fig. 12. Stress extension response in (a) brittle fracture and (b) ductile fracture.

discontinuous decrease in the stress to the value $W'(\mathcal{G}_{RQ}(\beta_F))$, followed by a continuous decrease as illustrated in Figure 12a. In ductile fracture, the stress increases to a maximum value $W'(\beta_P)$ and then decreases continuously as shown in Figure 12b.

6. DISCUSSION

The dichotomy between brittle and ductile fracture has been studied by several authors. For example, Needleman [17] considers a rectangular block with an imperfection in the form of a band of reduced stiffness and takes two incremental constitutive equations of the Kelvin-Voigt type, one for the block and one for the band. His model predicts the occurrence of ductile fracture when both of the instantaneous elastic moduli are negative and of brittle fracture when the modulus of the block is positive and that of the band is negative. The viscous moduli are taken to be equal, and their common value, as a parameter in the model, does not affect the type of fracture. In contrast, Carpinteri [18] develops Barenblatt's [5] cohesive crack model using a crack in place of a band: the constitutive equation for the crack is a relation between stress and jump in displacement determined by a concave, decreasing function similar to the function Θ' in the present theory. The use of a crack in place of a band permits one to predict a ductile-to-brittle transition that depends on a scale factor given by the length of the bar, as in the present analysis, whose presence has been confirmed in many experiments.

Another development of Barenblatt's ideas is due to Truskinovsky [19]. He replaces the bar by a finite chain of atoms, each connected to its nearest neighbors by a nonlinear spring obeying the Lennard-Jones law of atomic interactions. The resulting relation between stress and extension is similar to our Figure 12a, with the form of the lowest branch depending on the number of atoms in the chain in such a way that the lowest branch approaches the horizontal axis and the elongation β_F, marking the transition between the two branches, approaches zero

Downloaded from http://mms.sagepub.com at SIMON FRASER LIBRARY on November 11, 2008

as the number of atoms tends to infinity. Thus, in the limit, the material elongates indefinitely at zero stress. Truskinovsky attributes this undesired effect to the lack of an internal length scale in the model and examines ways of introducing such a scale.

The approach presented here shares with Carpinteri's model the feature of splitting the energy into two parts, one associated with bulk effects and the other with interfacial effects. Here, the scale factor l appears in (65), and its effect on the form of the branch $\mathcal{L}_c$ of the equilibrium loci in each of Figures 10 and 11 is embodied in relation (69). This effect agrees with a result of Schreyer and Chen [20], who considered the equilibrium of a strain-softening bar in the presence of an imperfection distributed over a band and studied the slope of the stress-strain curve in the neighborhood of the point β_P in our Figures 10, 11, and 12b. An advantage of the present model, as well as that of Truskinovsky, is that it does not assume that cracks or bands preexist; these two models predict the formation of cracks, in the sense that cracks provide energetically favorable alternatives to configurations without cracks.

Acknowledgments. The research of I. Fonseca was partially supported by the Army Research Office and the National Science Foundation, through the Center for Nonlinear Analysis (Department of Mathematical Sciences, Carnegie Mellon University), by the National Science Foundation under Grant No. DMS-9500531, and by the Max Planck Institute for Mathematics in the Sciences. The research of G. Del Piero was supported by a CNR grant within the Progetto Strategico Problemi della Progettazione Complessa. The research of D. Owen was supported by the National Science Foundation under Grant No. DMS-9703863.

REFERENCES

[1] Del Piero, G. and Owen, D. R.: Structured deformations of continua. *Arch. Rat. Mech. Anal.*, 124, 99–155 (1993).

[2] Del Piero, G. and Owen, D. R.: Integral-gradient formulae for structured deformations. *Arch. Rat. Mech. Anal.*, 131, 121–138 (1995).

[3] Owen, D. R.: Disarrangements in continua and the geometry of microstructure, in *Recent Advances in Elasticity, Viscoelasticity, and Inelasticity*, pp. 67–81, ed., K. Rajagopal, World Scientific, Singapore, 1995.

[4] Choksi, R. and Fonseca, I.: Bulk and interfacial energy densities for structured deformations of continua. *Arch. Rat. Mech. Anal.*, 138, 37–103 (1997).

[5] Barenblatt, G. I.: The formation of equilibrium cracks during brittle fracture: General ideas and hypotheses. Axially symmetric cracks. *Appl. Math. Mech. (PMM)*, 23, 622–636 (1959).

[6] Noll, W. and Virga, E.: Fit regions and functions of bounded variation. *Arch. Rat. Mech. Anal.*, 102, 1–22 (1988).

[7] Evans, L. C. and Gariepy, R. F.: *Measure Theory and Fine Properties of Functions*, CRC Press, Boca Raton, 1992.

[8] Ziemer, W. P.: *Weakly Differentiable Functions*, Springer, Berlin, 1989.

[9] De Giorgi, E. and Ambrosio, L.: Un nuovo tipo di funzionale del calcolo delle variazioni. *Atti Accademia Nazionale Lincei*, 82, 199–210 (1988).

[10] Alberti, G.: A Lusin type theorem for gradients. *J. Funct. Anal.*, 100, 110–118 (1991).

[11] Ambrosio, L.: Compactness for a special case of functions of bounded variation. *Bollettino Unione Matematica Italiana*, 3-B7, 857–881 (1989).

[12] Fonseca, I. and Müller, S.: Relaxation of quasiconvex functionals in $BV(\Omega; R^p)$ for integrands $f(x, u, \nabla u)$. *Arch. Rat. Mech. Anal.*, 123, 1–49 (1993).

[13] Nakanishi, F.: *Selected Papers*, eds., T. Okasaki, S. Kumagai, A. Watari, Y. Sato, K. Tsuda, and J. Shioiri. Department of Aeronautics, University of Tokyo, 1966.

[14] Grolig, G.: Plastische Deformation als Ausdruck Mikroskopischer Instabilität. Dissertation, Fachbereich Mechanik der Technischen Hochschule Darmstadt, 1985.

[15] Hill, R.: *The Mathematical Theory of Plasticity*, Oxford University Press, London, 1950.

[16] Taylor, G. I.: The mechanism of plastic deformation of crystals. Part I. Theoretical. *Proc. Roy. Soc., A*, 145, 362–387 (1934).

[17] Needleman, A.: On the competition between failure and instability in progressively softening solids. *J. Appl. Mech.*, 58, 294–296 (1991).

Downloaded from http://mms.sagepub.com at SIMON FRASER LIBRARY on November 11, 2008

[18] Carpinteri, A.: Cusp catastrophe interpretation of fracture instability. *J. Mech. Phys. Solids*, 37, 567–582 (1989).

[19] Truskinovsky, L.: Fracture as a phase transition, in *Contemporary Research in the Mechanics and Mathematics of Materials*, pp. 322–332, ed., R. C. Batra and M. F. Beatty, CIMNE, Barcelona, 1996.

[20] Schreyer, H. L. and Chen, Z.: One-dimensional softening with localization. *J. Appl. Mech.*, 53, 791–797 (1986).

[21] Del Piero, G. and Owen, D.: *Structured Deformations of Continua*, Lecture Notes, XXII Scuola Estiva di Fisica Matematica, Ravello, September 1997, forthcoming.

Downloaded from http://mms.sagepub.com at SIMON FRASER LIBRARY on November 11, 2008